

1 Photosynthetic sea slugs induce protective changes to 2 the light reactions of the chloroplasts they steal from 3 algae

4 Authors: Vesa Havurinne (vetahav@utu.fi), Esa Tyystjärvi (esatyy@utu.fi)

5 *University of Turku, Department of Biochemistry / Molecular plant biology, Finland*

6 Corresponding author: Esa Tyystjärvi, esatyy@utu.fi

7 Abstract

8 Sacoglossan sea slugs are able to maintain functional chloroplasts inside their own cells, and
9 mechanisms that allow preservation of the chloroplasts are unknown. We found that the slug *Elysia*
10 *timida* induces changes to the photosynthetic light reactions of the chloroplasts it steals from the alga
11 *Acetabularia acetabulum*. Working with a large continuous laboratory culture of both the slugs (>500
12 individuals) and their prey algae, we show that the plastoquinone pool of slug chloroplasts remains
13 oxidized, which can suppress reactive oxygen species formation. Slug chloroplasts also rapidly build up a
14 strong proton motive force upon a dark-to-light transition, which helps them to rapidly switch on
15 photoprotective non-photochemical quenching of excitation energy. Finally, our results suggest that
16 chloroplasts inside *E. timida* rely on oxygen-dependent electron sinks during rapid changes in light
17 intensity. These photoprotective mechanisms are expected to contribute to the long-term functionality
18 of the chloroplasts inside the slugs.

19 Introduction

20 The sea slug *Elysia timida* is capable of stealing chloroplasts from their algal prey (Figure 1). Once stolen,
21 the chloroplasts, now termed kleptoplasts, remain functional inside the slug's cells for several weeks,
22 essentially creating a photosynthetic slug. The only animals capable of this phenomenon are some
23 marine flatworms (Van Steenkiste et al., 2019) and sea slugs belonging to the Sacoglossan clade
24 (Rumpho et al., 2011; de Vries et al., 2014). Despite decades of research, there is still no consensus
25 about the molecular mechanisms that allow the slugs to discriminate other cellular components of the

26 algae and only incorporate the chloroplasts inside their own cells, or how the slugs maintain the
27 chloroplasts functional for times that defy current paradigms of photosynthesis. Also the question
28 whether the slugs in fact get a real nutritional benefit from the photosynthates produced by the stolen
29 chloroplasts, is still being debated (Cartaxana et al., 2017; Rauch et al., 2017).

30 One of the main problems that kleptoplasts face is light induced damage to both photosystems.
31 Photoinhibition of Photosystem II (PSII) takes place at all light intensities and photosynthetic organisms
32 have developed an efficient PSII repair cycle to counteract it (Tyystjärvi, 2013). Unlike higher plants
33 (Järvi et al., 2015), the chloroplast genomes of all algal species involved in long term kleptoplasty encode
34 FtsH, a protease involved in PSII repair cycle (de Vries et al., 2013). However, out of all prey algae
35 species of photosynthetic sea slugs, only in *Vaucheria litorea*, the prey alga of *Elysia chlorotica*, the
36 chloroplast-encoded FtsH contains the critical M41 metalloprotease domain required for degradation of
37 the D1 protein during PSII repair (Christa et al., 2018). Photoinhibition of Photosystem I (PSI) occurs
38 especially during rapid changes in light intensity (Tikkanen and Grebe, 2018) and should cause problems
39 in isolated chloroplasts in the long run. In addition to the specific inhibition mechanisms of the
40 photosystems, unspecific damage caused by reactive oxygen species (ROS) (Khorobrykh et al., 2020) is
41 expected to deteriorate an isolated chloroplast.

42 Photoprotective mechanisms counteract photodamage. Recent efforts have advanced our
43 understanding of photoprotection in kleptoplasts (Christa et al., 2018; Cartaxana et al., 2019). It has
44 been shown that kleptoplasts of *E. timida* do retain the capacity to induce physiological photoprotection
45 mechanisms similar to the ones in the prey green alga *Acetabularia acetabulum* (hereafter *Acetabularia*)
46 (Christa et al., 2018). The most studied mechanism is the "energy-dependent" qE component of non-
47 photochemical quenching of excitation energy (NPQ). qE is triggered through acidification of the
48 thylakoid lumen by protons pumped by the photosynthetic electron transfer chain. The xanthophyll
49 cycle enhances qE (Ruban and Horton, 1999; Papageorgiou and Govindjee, 2014) but there have been
50 contrasting reports on the capability of *E. timida* to maintain a highly functional xanthophyll cycle if the
51 slugs are not fed with fresh algae (i.e. starved) and about the effect of NPQ on kleptoplast longevity
52 (Christa et al., 2018; Cartaxana et al., 2019). Although advancing our understanding of the mechanisms
53 of kleptoplast longevity, these recent publications underline the trend of contradictory results that has
54 been going on for a long time.

55 There are reports of continuous husbandry of photosynthetic sea slugs, mainly *E. timida* (Schmitt et al.,
56 2014) and *E. chlorotica* (Rumpho et al., 2011), but still today most research is conducted on animals

57 caught from the wild. We have grown the sea slug *E. timida* and its prey *Acetabularia* in our lab for
58 several years (Figure 1). As suggested by Schmitt et al. (2014), *E. timida* is an attractive model organism
59 for photosynthetic sea slugs because it is easy to culture with relatively low costs (Figure 1E). A constant
60 supply of slugs has opened a plethora of experimental setups yet to be tested, one of the more exciting
61 ones being the case of red morphotypes of both *E. timida* and *Acetabularia* (Figure 1C,D). Red
62 morphotypes of *E. timida* and *Acetabularia* were first described by González-Wangüemert et al. (2006)
63 and later shown to be due to accumulation of an unidentified carotenoid during cold/high-light
64 acclimation of the algae that were then eaten by *E. timida* (Costa et al., 2012). The red morphotypes
65 provide a visual proof that the characteristics of the kleptoplasts inside *E. timida* can be modified by
66 acclimating their feedstock to different environmental conditions.

67 We optimized a new set of biophysical methods to study photosynthesis in the sea slugs and found
68 differences in photosynthetic electron transfer reactions between *E. timida* and *Acetabularia* grown in
69 varying culture conditions. The most dramatic differences between the slugs and their prey were
70 noticed in PSII electron transfer of the red morphotype *E. timida* (Figure 1C) and *Acetabularia* (Figure
71 1D). In addition to measuring chlorophyll *a* fluorescence decay kinetics, we also measured fluorescence
72 induction kinetics, PSI electron transfer and formation of proton motive force during dark to light
73 transition. Our results suggest that dark reduction of the plastoquinone (PQ) pool, a reserve of central
74 electron carriers of the photosynthetic electron transfer chain, is weak in the slugs compared to the
75 algae, and that a strong build-up of proton motive force is likely linked to higher levels of NPQ in
76 kleptoplasts. It is also clear that PSI utilizes oxygen sensitive electron sinks in both the slugs and the
77 algae, and this sink protects the photosynthetic apparatus from light-induced damage in *E. timida*.

78 Results

79 Non-photochemical reduction of the chloroplast electron transfer chain is inefficient in *E.* 80 *timida*

81 We estimated reoxidation kinetics of the first stable electron acceptor of PSII, Q_A^- , from dark acclimated
82 *E. timida* and *Acetabularia* by measuring the decay of chlorophyll *a* fluorescence yield after a single
83 turnover flash (Figure 2). In the green morphotypes of the slugs and the algae, Q_A^- reoxidation kinetics
84 were similar between the two species in aerobic conditions both in the absence and presence of 3-(3, 4-
85 dichlorophenyl)-1, 1-dimethylurea (DCMU), an inhibitor of PSII electron transfer (Figure 2A,B). This
86 indicates that electron transfer within PSII functions in the same way in both species. In anaerobic

87 conditions, fluorescence decay was slower than in aerobic conditions in both species (Figure 2C),
88 showing that the environment of the slug kleptoplasts normally remains aerobic in the dark even in the
89 presence of slug respiration. Anaerobicity slowed the fluorescence decay less in *E. timida* than in
90 *Acetabularia*, especially during the fast ($\sim 300\text{--}500\ \mu\text{s}$) and middle ($\sim 5\text{--}15\ \text{ms}$) phases of fluorescence
91 decay in anaerobic conditions (Figure 2C). Decay of fluorescence is slow in anaerobic conditions likely
92 because dark reduction of the electron transfer chain, specifically the PQ pool, hinders Q_A^- reoxidation
93 (de Wijn and van Gorkom, 2001; Oja et al., 2011; Deák et al., 2014; Krishna et al., 2019). This suggests
94 that non-photochemical reduction of the electron transfer chain during the dark acclimation period is
95 less efficient in the slug than in the alga.

96 The decay of fluorescence after a single turnover flash followed strong wave like kinetics in the red
97 morphotype *Acetabularia*, with a large undershoot below the dark-acclimated minimum fluorescence
98 level, while there was no sign of such kinetics in the red morphotype *E. timida* (Figure 2D, see also Figure
99 1C,D for images of the red morphotypes and “Materials and methods” for their preparation). The wave
100 phenomenon has been characterized in detail in several species of cyanobacteria, where anaerobic
101 conditions in the dark are enough for its induction (Wang et al., 2012; Deák et al., 2014; Ermakova et al.,
102 2016). According to Deák et al., (2014), anaerobic conditions cause a highly reduced PQ pool through
103 respiratory electron donation, mainly from NAD(P)H. This reduction is mediated by the NAD(P)H-
104 dehydrogenase (NDH). Taken together, the results shown in Figure 2C, D indicate that the dark
105 reduction of the chloroplast’s electron transfer chain is not as strong in *E. timida* as it is in *Acetabularia*.

106 Full photochemical reduction of the electron transfer chain during a dark-to-light 107 transition is delayed in *E. timida*

108 In order to investigate whether the alterations in the dark reduction of the electron transfer chain in
109 kleptoplasts lead to differences in electron transfer reactions during continuous illumination, we
110 measured chlorophyll *a* fluorescence induction kinetics from both *E. timida* and *Acetabularia* (Figure 3).
111 Briefly, fluorescence rise during the first $\sim 1\ \text{s}$ of continuous illumination of a photosynthetic sample can
112 be divided into distinct phases, denoted as O-J-I-P, when plotted on a logarithmic time scale (see Figure
113 3A). Alterations in the magnitude and time requirements of these phases are indicative of changes in
114 different parts of the photosynthetic electron transfer chain (Strasser et al., 1995; Strasser et al., 2004;
115 Kalaji et al., 2014).

116 Fluorescence induction measurements in aerobic conditions revealed that in green *E. timida* individuals
117 maximum fluorescence (P phase of OJIP fluorescence rise kinetics) was reached ~300 ms later than in
118 green *Acetabularia* (Figure 3A). To investigate whether the elongated time requirement to reach
119 maximum fluorescence is caused by light attenuation in the slug tissue, we tested the effect of different
120 intensities of the light pulse to the fluorescence transient in *E. timida*. In the tested range, the intensity
121 of the pulse did affect the O-J-I phases but not the time of the P phase in aerobic conditions (Figure 3 -
122 figure supplement 1). This suggests that the ~300 ms delay of the P phase in *E. timida* is of physiological
123 origin, and once again an indicator of differing redox poises of the chloroplasts between *E. timida* and
124 *Acetabularia*.

125 We witnessed a slightly slower O-J phase in DCMU treated *E. timida* individuals (~10 ms to reach J) than
126 in DCMU treated *Acetabularia* (~6 ms) (Figure 3B). The O-J phase is considered to represent the
127 reduction of Q_A to Q_A^- , and it is indicative of the amount of excitation energy reaching PSII, i.e. functional
128 absorption cross-section of the PSII light harvesting antennae (Kalaji et al., 2014). The J-I-P phases are
129 nullified when DCMU is introduced into the sample, as forward electron transfer from Q_A^- is blocked
130 (Kodru et al., 2015), which makes the O-J phase highly distinguishable. While it is conceivable that the
131 slower O-J fluorescence rise (Figure 3B) indicates a decrease in the functional absorption cross-section
132 of PSII in the slug cells, artefactual changes to the fluorescence signal by the different optical properties
133 of the slugs and the algae cannot be ruled out as an explanation for the minute difference (~4 ms) in the
134 O-J phase based on the current data. Comparison of the differing photosynthetic matrices between the
135 slugs and the algae, and their effects on the photosynthetic parameters derived from fluorescence
136 measurements have been thoroughly discussed in Cruz et al., (2013) and Serôdio et al., (2014). We
137 cannot completely rule out the possibility that DCMU does not block all PSII units of the kleptoplasts but
138 find this unlikely, as addition of DCMU caused a similar change in the form of the OJIP curve in both
139 slugs and algae (Figs. 3A and 3B).

140 In anaerobic conditions the OJIP transient behaved in a manner that can be explained by a highly
141 reduced electron transfer chain (Figure 3C). This blockage seems to affect the electron transfer more in
142 *Acetabularia* than in *E. timida*, i.e. the J-I-P phases are more pronounced in *E. timida*, supporting the
143 earlier suggestion derived from Figure 2C, that in anaerobic conditions electron transfer from Q_A^- to Q_B
144 and PQ pool is faster in *E. timida* than in *Acetabularia*.

145 Chloroplasts in *E. timida* exhibit strong build-up of proton motive force in the light

146 To inspect intricate differences in proton motive force formation between *E. timida* and *Acetabularia*,
147 we measured electrochromic shift (ECS) from dark acclimated individuals of both species during a
148 strong, continuous light pulse (Figure 4A). According to the ECS data, proton motive force of
149 *Acetabularia* dissipates to a steady level after the initial spike in thylakoid membrane energization,
150 whereas in *E. timida* there is a clear build-up of proton motive force after a slight relaxation following
151 the initial spike. ECS was also measured from *E. timida* individuals that were devoid of kleptoplasts, and
152 the slug tissue itself was found not to cause any inherent distortions to the ECS signal (Figure 4 – figure
153 supplement 1).

154 *E. timida* and *Acetabularia* utilize oxygen dependent electron sinks from PSI

155 We utilized a nearly identical protocol as Shimakawa et al. (2019) to measure redox kinetics of P700, the
156 reaction center chlorophyll of PSI, in dark acclimated *E. timida* and *Acetabularia* during dark-to-light
157 transition (Figure 4B-D, see also Figure 4 – figure supplement 1C for P700 redox kinetics measurements
158 from *E. timida* individuals without any kleptoplasts). In aerobic conditions, *Acetabularia* P700 redox
159 kinetics during a high-light pulse followed the scheme where P700 is first strongly oxidized due to PSI
160 electron donation to downstream electron acceptors such as ferredoxin, and re-reduced by electrons
161 from the upstream electron transfer chain (Figure 4B). Finally, oxidation is resumed by alternative
162 electron acceptors of PSI, most likely FLVs, as they have been shown to exist in all groups of
163 photosynthetic organisms except angiosperms and certain species belonging to the red-algal lineage
164 (Allahverdiyeva et al., 2015; Ilík et al., 2017; Shimakawa et al., 2019). P700 redox kinetics in *E. timida* and
165 *Acetabularia* in aerobic conditions were similar in terms of the overall shape of the curve, but the re-
166 oxidation phase after ~600 ms was dampened in *E. timida* (Figure 4B). In the presence of DCMU, P700
167 remained oxidized throughout the pulse in both species (Figure 4C). Data concerning non-photochemical
168 reduction of P700⁺ after the light pulse in the presence of DCMU are heavily affected by the
169 normalization process of the signal in *E. timida*, and therefore minor fluctuations of the signal cannot be
170 taken as evidence for physiological phenomena. The DCMU data does, however, show that the re-
171 reduction of P700⁺ after the initial peak in aerobic conditions (Figure 4B) is due to electron donation
172 from PSII in *E. timida* and *Acetabularia*, which further validates the method. The final oxidation phase
173 was absent in both species in anaerobic conditions (Figure 4D), indicating that both *E. timida* and
174 *Acetabularia* utilize oxygen-dependent alternative electron sinks functioning after PSI to maintain P700
175 oxidized.

176 During the optimization process of the P700 oxidation measurements, we found that firing a second
177 high-light pulse 10 s after the first pulse resulted in a higher capacity to maintain P700 oxidized in both
178 *E. timida* and *Acetabularia* in aerobic conditions (Figure 4B, inset). This procedure will hereafter be
179 referred to as “second pulse protocol”. In *E. timida* the oxidation capacity was moderate even with the
180 second pulse, showing a high re-reduction of P700⁺ after the initial oxidation. In *Acetabularia* the second
181 pulse rescued P700 oxidation capacity completely. When a second pulse was fired in anaerobic
182 conditions, P700 oxidation capacity showed only weak signs of improvement in *E. timida* and
183 *Acetabularia* (Figure 4D, inset).

184 P700 redox kinetics in *E. timida* are affected by the acclimation status of its prey

185 We tested the sensitivity of *E. timida* P700⁺ measurements by inflicting changes to the P700 oxidation
186 capacity of its prey, and then estimating whether the changes are present in the slugs after feeding
187 them with differently treated *Acetabularia*. First, we grew *Acetabularia* in elevated (1 %) CO₂
188 environment, as high CO₂ induces downregulation of the main alternative electron sinks of PSI, FLVs, in
189 cyanobacteria and green algae (Zhang et al., 2012; Jokel et al., 2015; Santana-Sanchez et al., 2019). Next,
190 we allowed *E. timida* to feed on high-CO₂ *Acetabularia* for four days. We used *E. timida* individuals that
191 had been pre-starved for four weeks to ensure that the slugs would only contain chloroplasts from high-
192 CO₂ *Acetabularia*. After feeding, the slugs were allowed to incorporate the chloroplasts into their own
193 cells for an overnight dark period in the absence of *Acetabularia* prior to the measurements. A similar
194 treatment was applied to slug individuals that were fed ambient-air grown *Acetabularia* (see “Materials
195 and methods” for the differences in the feeding regimes). These slugs will hereafter be termed as high-
196 CO₂ and ambient-air *E. timida*, respectively.

197 Ambient-air *E. timida* exhibited stronger P700 oxidation during the initial dark-to-light transition than
198 high-CO₂ *E. timida* (Figure 5A). When the second pulse protocol was applied, both groups showed a clear
199 increase in P700 oxidation capacity, but once again P700 oxidation was stronger in the ambient-air slugs
200 (Figure 5C). The differences between ambient-air and high-CO₂ *Acetabularia* showed the same trend
201 (Figure 5B,D). Acclimation to high CO₂ also caused changes to PSII activity, estimated as relative electron
202 transfer of PSII (rETR) during rapid light curve (RLC) measurements from dark acclimated samples (Figure
203 5E,F). Maximal rETR was lower in ambient-air *E. timida* and *Acetabularia* than in their high-CO₂
204 counterparts. Also the behaviour of NPQ during the RLC measurements indicated that ambient-air and
205 high-CO₂ *E. timida* had very similar photosynthetic responses as their respective food sources (Figure
206 5G,H). However, the slugs did exhibit higher levels of NPQ than the algae in both cases.

207 As regulation of FLVs in response to CO₂ conditions might explain the differences in P700 redox kinetics
208 (Zhang et al., 2012; Jokel et al., 2015; Santana-Sanchez et al., 2019), we confirmed their presence in
209 *Acetabularia* by Western blotting (Figure 6), using an antibody raised against *Chlamydomonas*
210 *reinhardtii* FLVB; the antibody also reacts with FLVA of *C. reinhardtii* (Jokel et al., 2015). This antibody
211 recognized one protein band of approximately 60 kDa size in *Acetabularia*, falling to the size range of
212 FLVs from *C. reinhardtii* (70 and 58 kDa for FLVA and FLVB, respectively; Figure 6B). Our results show
213 that there was no significant difference in FLV amounts between ambient air and high-CO₂ *Acetabularia*
214 (Figure 6A; Student's t-test, P=0.594, n=3), suggesting that CO₂ concentration does not regulate FLVs at
215 the protein level in *Acetabularia*. However, the FLV-specific band of *Acetabularia* was wider than the
216 Coomassie stained band (Fig. 6C), possibly indicating that the antibody reacted with multiple proteins of
217 similar molecular weight. In *C. reinhardtii*, the Coomassie stain and Western blot produced a similar
218 FLVB band, but Coomassie staining did not reveal the FLVA band (Fig. 6C).

219 High-CO₂ *E. timida* kleptoplasts are sensitive to fluctuating light

220 Recently, there has been an increasing interest in protection of PSI by alternative electron sinks such as
221 FLVs (Shimakawa et al., 2019; Gerotto et al., 2016; Jokel et al., 2018). This led us to investigate whether
222 P700 oxidation capacity would affect the longevity of the kleptoplasts. We first compared kleptoplast
223 longevity in ambient-air and high-CO₂ *E. timida* in starvation under normal day/night cycle (12/12h,
224 PPFD 40 $\mu\text{mol m}^{-2}\text{s}^{-1}$ during daylight hours), i.e. steady-light conditions. The slugs used here were
225 subjected to a 4 week pre-starvation protocol prior to feeding them with their respective algae before
226 the onset of the actual steady-light starvation experiment (see "P700 redox kinetics in *E. timida* are
227 affected by the acclimation status of its prey" and "Materials and methods" for details).

228 Both groups behaved very similarly in terms of slug coloration and size, maximum quantum yield of PSII
229 photochemistry (F_V/F_M) and minimal and maximal chlorophyll fluorescence (F_0 and F_M , respectively)
230 during a 46 day starvation period (Figure 7). Both F_0 and F_M decreased during starvation (Fig. 7D) but as
231 several factors, including photoinhibition of PSII (Tyystjärvi, 2013), quenching of excitation energy by
232 photoinhibited PSII (Matsubara and Chow, 2004) and the overall decrease of kleptoplasts during
233 starvation affect these values, all conclusions will be based on the F_V/F_M ratio. In both groups, F_V/F_M
234 decreased during starvation in a bi-phasic pattern, with slow decrease until day 21, after which PSII
235 activity declined rapidly. The overall decline in F_V/F_M was nearly identical in both groups throughout the
236 experiment (Figure 7C). The initial population size of both groups was 50 slugs, and starvation induced
237 deaths of 9 and 12 slugs during the experiment from ambient-air and high-CO₂ *E. timida* populations,

238 respectively (see “Materials and methods” for details on mortality and sampling). P700⁺ measurements
239 from slugs starved for 5 days indicated that the starved ambient-air *E. timida* retained a higher P700
240 oxidation capacity through starvation than high-CO₂ *E. timida*, when the second pulse P700⁺ kinetics
241 protocol was applied (Figure 7E). These results show that altered P700 oxidation capacity does not
242 affect chloroplast longevity in *E. timida* in steady-light conditions.

243 We repeated the starvation experiment with new populations of ambient-air and high-CO₂ *E. timida*, but
244 this time the moderate background illumination (PPFD 40 $\mu\text{mol m}^{-2}\text{s}^{-1}$) was supplemented every 10 min
245 with a 10 s high-light pulse (PPFD 1500 $\mu\text{mol m}^{-2}\text{s}^{-1}$) during daylight hours, i.e. fluctuating light. Slugs
246 used in this experiment were not subjected to a pre-starvation protocol prior to feeding them with their
247 respective algae but were simply allowed to replace their old chloroplasts with new specific ones during
248 6 days of feeding. The starting population size was 45 slugs for both groups and there were no
249 starvation-caused losses during the whole experiment (see “Materials and methods” for details on
250 sampling).

251 Starvation in fluctuating light induced faster onset of the rapid phase of F_V/F_M decrease in both groups
252 (Figure 8A) when compared to the steady light starvation experiment (Figure 7C). The exact onset of the
253 rapid decline of F_V/F_M was difficult to distinguish, but in ambient-air *E. timida* F_V/F_M decrease accelerated
254 only after ~20 days, whereas in high-CO₂ *E. timida* the turning point was during days 10-14 (Figure 8A).
255 The overall longevity of PSII photochemistry in both groups was, however, very similar, as there was a
256 sudden drop in F_V/F_M in the ambient-air slugs on day 31. F_0 behaved identically in the two groups, apart
257 from days 0-4, when F_0 of the high-CO₂ *E. timida* dropped to the level of the ambient-air *E. timida* F_0 . At
258 day 10, F_M of the high-CO₂ slugs dropped drastically and the groups started to differ. Using the second
259 pulse P700⁺ measurement protocol, we confirmed that the differences in P700 oxidation capacity were
260 noticeable on days 0 and 6 in starvation also in the populations of slugs used for the fluctuating-light
261 experiment (Figure 8C,D). RLC measurements were performed on the slugs on day 10 to inspect the
262 underlying causes of the suddenly decreasing fluorescence parameters F_V/F_M and F_M of the high-CO₂
263 slugs (Figure 8E). The situation after 10 days in fluctuating light seemed almost the opposite to the
264 situation on day 0 (Figure 5E), i.e. now the ambient-air slugs showed higher $rETR_{MAX}$ than the high-CO₂
265 slugs (Figure 8E). However, the behaviour of NPQ during the RLC measurements showed that high-CO₂
266 *E. timida* were still able to generate and maintain stronger NPQ than ambient-air *E. timida* (Figure 8F,
267 Figure 8- figure supplement 1), although the differences were not as strong as on day 0 (Figure 5G).
268 These data indicate that the initial chloroplast acclimation status is retained during starvation, and the

269 decrease in $rETR_{MAX}$ in high- CO_2 *E. timida* is likely due to light induced damage to the photosynthetic
270 apparatus.

271 Discussion

272 Weakened dark reduction of the PQ pool lowers electron pressure in *E. timida* 273 kleptoplasts

274 Our data on Chl fluorescence relaxation (Figure 2) and induction kinetics (Figure 3) reveal differences in
275 the dark and light reduction of the photosynthetic electron transfer chain between chloroplasts inside *E.*
276 *timida* and *Acetabularia*. While the connection between fluorescence transients and specific redox
277 components of the electron transfer chain are still under debate, especially concerning the J-I-P phase of
278 the OJIP curves (Stirbet and Govindjee, 2012; Schansker et al., 2014; Vredenberg, 2015; Havurinne et al.,
279 2018; Magyar et al., 2018; Schreiber et al., 2019), our data suggest that the differences in the redox
280 behavior between the slugs and the algae specifically reflect differences in the redox state of the PQ
281 pool.

282 The strongest indicators of differences in dark reduction of the PQ pool between the slugs and the algae
283 are the Q_A^- reoxidation measurements from the red morphotype *E. timida* and *Acetabularia* (Figure 2D).
284 Red morphotype *Acetabularia* exhibited clear wave like kinetics of fluorescence decay, while the wave
285 was completely absent in red *E. timida*. The wave phenomenon was recently characterized in the green
286 alga *C. reinhardtii* (Krishna et al., 2019). The authors suggested that, similar to cyanobacteria, non-
287 photochemical reduction of the PQ pool by stromal reductants in anaerobic conditions in the dark leads
288 to wave like kinetics of fluorescence decay after a single turnover flash in sulphur deprived *C. reinhardtii*
289 cells. The exact mechanisms underlying the wave phenomenon are still unknown, but the involvement
290 of NDA2, a type II NDH protein is clear (Deák et al., 2014; Krishna et al., 2019). Chemical inhibition of
291 NDA2 in *C. reinhardtii* led to complete abolishment of the wave phenomenon in cells that were
292 otherwise primed for it (Krishna et al., 2019). Interestingly, the comparison of NDA2 uninhibited and
293 inhibited cells resulted in fluorescence decay kinetics that are highly reminiscent of the kinetics in Figure
294 2D, with the red morphotype *E. timida* and red morphotype *Acetabularia* being analogous to the NDA2
295 inhibited and uninhibited *C. reinhardtii* cells, respectively. Despite the remarkable analogy, more
296 experiments are needed to validate the presence of a type II NDH protein in *Acetabularia* and its role in
297 the wave-phenomenon in the red morphotype. However, since there are no reports indicating
298 incorporation of algal mitochondria by Sacoglossan sea slugs and they have been shown to digest

299 cellular components of the algae other than the chloroplasts (Rumpho et al., 2000), we interpret the
300 lack of the wave phenomenon as a sign of missing contribution of respiratory electron donors into the
301 kleptoplasts inside *E. timida*. Either *E. timida* kleptoplasts are completely cut off from respiratory
302 electron donors deriving from the slug's own mitochondria, or they are not delivered into the PQ pool
303 due to inhibition of a type II NDH protein. The Q_A^- reoxidation data in Figure 2C, showing that
304 fluorescence decay is faster in *E. timida* than in *Acetabularia* in anaerobic conditions, indicate that dark
305 reduction of the PQ pool is weakened also in regular green *E. timida* individuals.

306 The weakened dark reduction of the PQ pool in *E. timida* has consequences to photosynthetic electron
307 transfer in the light. The ~300 ms delay in reaching the maximum fluorescence during the OJIP
308 measurements in *E. timida* in Figure 3A indicates that the PQ pool is more oxidized in the slugs than in
309 *Acetabularia* even in aerobic conditions, and full reduction of the PQ pool simply takes longer in *E.*
310 *timida*. We base this on the notion that full reduction of the PQ pool is a prerequisite for reaching
311 maximum fluorescence when fluorescence rise kinetics are measured using multiple turnover saturating
312 light pulses, such as the ones used in the current study (Kramer et al., 1995; Yaakoubd et al., 2002;
313 Suggett et al., 2003; Osmond et al., 2017). Maintaining an oxidized PQ pool could be advantageous for
314 chloroplast longevity, as it would help mitigate electron pressure and ROS formation in PSII.

315 Build-up of proton motive force in *E. timida* may facilitate strong NPQ

316 We witnessed a clear increase in proton motive force during a high light pulse in *E. timida*, whereas in
317 *Acetabularia* proton motive force relaxes considerably after the initial spike in thylakoid membrane
318 energization (Figure 4A). The build-up of proton motive force in *E. timida* suggests that protons are
319 released into the thylakoid lumen during illumination, but not out. This could be indicative of defects in
320 ATP-synthase functionality in the slugs, perhaps due to lack of inorganic phosphate. Interestingly, our
321 results from ambient air and high-CO₂ slugs and algae show that while the acclimation state of the prey
322 algae is reflected onto the NPQ capacity of the slugs, the slugs exhibit higher levels of NPQ than their
323 respective prey *Acetabularia* at the same light intensities (Figure 5G,H). Similar data has previously been
324 presented from *E. timida* and also *E. chlorotica* (Cruz et al., 2015; Christa et al., 2018). Higher level of
325 NPQ in the slugs is likely linked to the strong acidification of the lumen in the slugs (Figure 4A), since the
326 major qE component of NPQ is pH dependent (Müller et al., 2001; Papageorgiou and Govindjee, 2014).
327 The xanthophyll cycle of freshly fed *E. timida* is functional (Cartaxana et al., 2019), but it is unclear
328 whether the NPQ induced already during the first 100 s of the RLC measurement (Figure 5G) is due to
329 lumen acidification switching on the xanthophyll cycle, or whether lumen acidification directly enhances

330 quenching capacity at the level of light harvesting antennae. Nevertheless, strong NPQ has obvious
331 benefits for chloroplast longevity in *E. timida*.

332 Flavodiiron proteins function as alternative electron sinks in *E. timida* and *Acetabularia*

333 *E. timida* and *Acetabularia* utilize oxygen-dependent electron acceptors of PSI during dark-to-light
334 transition, but their functionality is weaker in *E. timida* (Figure 4B-C). Based on the current literature on
335 P700 redox kinetics during the first seconds after a dark to light transition, the most likely candidates for
336 these electron acceptors are FLVs that donate electrons to oxygen (Jokel et al., 2015; Gerotto et al.,
337 2016; Ilík et al., 2017; Jokel et al., 2018; Shimakawa et al., 2019). Indeed, the presence of FLVs was also
338 confirmed in *Acetabularia* by Western blotting (Figure 6). Using the second pulse protocol for P700
339 redox measurements, we showed that P700 oxidation capacity increases after the initial pulse of light in
340 both *E. timida* and *Acetabularia* (Figure 4B). Full activation of FLVs as electron acceptors of PSI takes ~1s
341 after a transition from dark to light and they subsequently remain a considerable electron sink during
342 the time required for light activation of Calvin-Benson-Bassham cycle (Ilík et al., 2017; Gerotto et al.,
343 2016; Bulychev et al., 2018). The mechanism of such fast regulation of FLV functionality is not known,
344 but the conserved cysteine residues of FLVs have been suggested to offer a means for redox regulation
345 through conformational changes (Alboresi et al., 2019). This, in conjunction with the data showing that
346 anaerobicity diminishes P700 reoxidation even with the second pulse protocol (Figure 4D), support the
347 view that FLVs are also behind P700 oxidation during the second pulse.

348 High P700 oxidation capacity improves kleptoplast longevity under fluctuating light

349 By feeding *E. timida* individuals with *Acetabularia* grown in ambient air and high CO₂ conditions, we
350 successfully created slugs whose kleptoplasts reflected the acclimation state of their respective prey
351 algae at the levels of P700 redox kinetics (Figure 5A-D), rETR (Figure 5E,F) and NPQ (Figure 5G,D).
352 Acclimation to high CO₂ led to a noticeable decrease in P700 oxidation capacity in both *Acetabularia* and
353 *E. timida* (Figure 5A-D). The simplest explanation for this is downregulation of FLVs in elevated CO₂
354 environment (Jokel et al., 2015), but this was not confirmed by a Western blot analysis from ambient-air
355 and high-CO₂ *Acetabularia* (Figure 6A). However, the protein band detected with the FLV antibody from
356 *Acetabularia* is broad, and might conceal two protein bands, possibly the *Acetabularia* homologues of
357 FLVA and FLVB. Another important factor influencing PSI electron transfer that could be affected by
358 alterations in CO₂ levels in *Acetabularia* is the Mehler's reaction, but this seems an unlikely candidate for
359 the differences in P700 redox kinetics during the 780 ms light pulse, as the evidence from FLV knockout
360 and insertion mutant algae and plants show that Mehler's reaction cannot substitute for FLVs in the

361 reoxidation of P700 during such a time frame (Gerotto et al., 2016; Ilík et al., 2017; Jokel et al., 2018).
362 Also altered stoichiometry of PSII and PSI could affect P700 redox kinetics, but the highly similar ratio of
363 chlorophylls *a* and *b* between ambient-air (chlorophyll *a/b*=2.37, SE±0.03, n=5) and high-CO₂ slugs
364 (chlorophyll *a/b*=2.41, SE±0.06, n=6) indicates that photosystem stoichiometry does not strongly depend
365 on CO₂ concentration. Whatever the exact reason behind the altered P700 redox kinetics is, it is clear
366 that acclimation of *Acetabularia* to high CO₂ lowers P700 oxidation capacity and this acclimation state is
367 transferred into *E. timida*.

368 When ambient air and high-CO₂ *E. timida* were starved for 46 days in steady-light conditions, they
369 behaved nearly identically in terms of kleptoplast longevity, while still retaining the differences in P700
370 redox kinetics after 5 days in starvation (Figure 7). The differences in P700 redox kinetics were also
371 noticeable on days 0 and 6 of the starvation experiment in fluctuating light. In fluctuating light, F_V/F_M of
372 the high-CO₂ slugs decreased faster than in ambient-air slugs (Figure 8). Our results suggest that
373 alternative electron acceptors of PSI, possibly FLVs, are utilized by *E. timida* to protect kleptoplasts from
374 formation of ROS during fluctuating-light starvation. The exact mechanism of PSI damage is not clear,
375 but FLVs have been shown to protect PSI in green algae by donating excess electrons to oxygen without
376 producing ROS (Shimakawa et al., 2019; Jokel et al., 2018). However, both slug groups did retain PSI
377 activity for at least up to 6 days in starvation (Figure 8D). This shows that PSI was protected against
378 fluctuating light even in the high-CO₂ *E. timida* that exhibited lowered, but not completely abolished,
379 P700 oxidation capacity. Lower P700 oxidation capacity in high-CO₂ slugs could, however, cause an
380 increase in the rate of Mehler's reaction (Mehler, 1951; Khorobrykh et al., 2020). Superoxide anion
381 radical and hydrogen peroxide, the main ROS produced by Mehler's reaction, are not likely to be
382 involved in the primary reactions of PSII photoinhibition but are known to have deleterious effects on
383 PSII repair (Tyystjärvi, 2013). We propose that this is behind the faster decrease in F_V/F_M and rETR in the
384 high-CO₂ *E. timida* in fluctuating light.

385 Conclusions

386 We have performed the most detailed analysis of the differences in photosynthetic light reactions
387 between a photosynthetic sea slug and its prey alga to date. Our results indicate that in the dark the PQ
388 pool of the kleptoplasts inside the sea slug *E. timida* is not reduced to the same extent as in chloroplasts
389 inside the green alga *Acetabularia* (Figure 2). Fluorescence induction measurements also suggest that
390 there are differences in the PQ pool redox state between kleptoplasts in *E. timida* and chloroplasts in
391 *Acetabularia*. The considerable delay in reaching the maximum chlorophyll *a* fluorescence in *E. timida*

392 during a high-light pulse (Figure 3A) can be indicative of a highly oxidized PQ pool that simply takes
 393 longer to fully reduce.

394 Our results show that oxidation of P700 seems to be weaker in *E. timida* than in *Acetabularia* (Figure 4B,
 395 Figure 5 A-D), but still enough to offer protection from light-induced damage in fluctuating light in *E.*
 396 *timida* (Figure 8). If the capacity to oxidize P700 by alternative electron acceptors is lowered in *E. timida*
 397 kleptoplasts, is this compensated for by an increased capacity of the main electron sink, i.e. the Calvin-
 398 Benson-Bassham cycle? If not, *E. timida* slugs would risk having a foreign organelle inside their own cells
 399 that readily produces ROS via one-electron reduction of oxygen. Interestingly, a major feature
 400 separating Sacoglossan slug species capable of long-term retention of kleptoplasts from those that are
 401 not, is their high capacity to downplay starvation induced ROS accumulation (de Vries et al., 2015). This
 402 could imply that long-term retention slug species such as *E. timida* do not need to concern themselves
 403 over the perfect functionality of the electron transfer reactions downstream of PSI. Further in-depth
 404 investigations into the carbon fixation reactions in photosynthetic sea slugs are needed to test this
 405 hypothesis. In addition to bringing closure to a biological conundrum that has remained unanswered for
 406 decades, solving how sea slugs are able to incorporate and maintain kleptoplasts in their own cells could
 407 provide useful insights into the ancient endosymbiotic events that led to the evolution of eukaryotic life.

408 Materials and methods

Key Resources Table				
Reagent type (species) or resource	Designation	Source or reference	Identifiers	Additional information
strain, strain background (<i>Elysia timida</i>)	<i>Elysia timida</i> Turku Isolate1 (T11)	This paper		Mediterranean locality (Elba, Italy, 42.7782° N, 10.1927° E)
strain, strain background (<i>Acetabularia acetabulum</i>)	<i>Acetabularia acetabulum</i> Düsseldorf Isolate 1 (DI1)	This paper, Schmitt et al., 2014		Mediterranean locality, strain originally isolated by

				Diedrik Menzel
biological sample (<i>Chlamydomonas reinhardtii</i>)	CC406 wild-type strain	Jokel et al., 2015; Chlamydomonas resource center	RRID:SCR_014960	Total protein extract
antibody	Rabbit anti-FLVB	Jokel et al., 2015		(1:5000)
commercial assay or kit	DC™ Protein Assay Kit	Bio-Rad	Bio-Rad #5000111	
commercial assay or kit	Next Gel 10% Polyacrylamide Gel Electrophoresis Solutions	VWR	VWR # 97063-026	
chemical compound, drug	3-(3, 4-dichlorophenyl)-1, 1-dimethylurea (DCMU)	Merck	Merck #D2425	
chemical compound, drug	D-(+)-Glucose	Merck	Merck #G8270	
chemical compound, drug	Glucose Oxidase from <i>Aspergillus niger</i>	Merck	Merck #G2133	
chemical compound, drug	Catalase from bovine liver	Merck	Merck #C9322	
software, algorithm	Fiji	Schindelin et al., 2012	RRID:SCR_003070	
software, algorithm	Origin	Originlab (https://originlab.com)	RRID:SCR_014212	Origin 2016 v.9.3

409

410 Organisms and culture conditions

411 Axenic stock cultures of the green alga *Acetabularia* (Düsseldorf Isolate 1, DI1; strain originally isolated
412 by Diedrik Menzel) were grown in 5-10 l plastic tanks in sterile filtered f/2 culture medium made in 3.7 %
413 artificial sea water (ASW; Sea Salt Classic, Tropic Marin, Montague, MA, USA). All ASW was prepared in
414 10 l batches in regular tap water of Turku, Finland. It is important to note the regional differences in tap
415 water quality, and the suitability of tap water for cultures of algae or sea slugs should be assessed
416 before large scale cultures to avoid mass loss of the cultures. In order to slow down the stock culture
417 growth, PPFD of growth lights (TL-D 58W/840 New Generation fluorescent tube; Philips, Amsterdam,
418 The Netherlands) was $<20 \mu\text{mol m}^{-2}\text{s}^{-1}$. The culture medium for the stock cultures was changed at 8-10
419 week intervals. Keeping the lids of the *Acetabularia* tanks locked in place (Figure 1E) effectively
420 prevented excessive evaporation from the tanks. Other *Acetabularia* culture maintenance procedures,
421 such as induction of gamete release, formation of zygotes and sterilization procedures were performed
422 essentially as described earlier (Hunt and Mandoli, 1992; Cooper and Mandoli, 1999). The day-night
423 cycle was 12/12 h and temperature was maintained at 23 °C at all times for all algae and slug cultures,
424 unless mentioned otherwise. Algae used in the experiments were transferred to new tanks containing
425 fresh f/2 media and grown under lights adjusted to PPFD $40 \mu\text{mol m}^{-2}\text{s}^{-1}$ (TL-D 58W/840 New Generation
426 fluorescent tube) for minimum of two weeks prior to any further treatments. No attempt was made to
427 use only algae of certain age or size, and all populations were mixtures of cells in different
428 developmental stages. PPFD was measured with a planar light sensor (LI-190R Quantum Sensor; LI-COR
429 Biosciences; Lincoln, NE, USA) at the tank bottom level in all growth and treatment conditions.
430 Irradiance spectra of all growth light sources used in the current study are shown in Figure 6 – figure
431 supplement 1, measured with an absolutely calibrated STS-VIS spectrometer (Ocean Optics, Largo, FL,
432 USA).

433 Sea slug *E. timida* individuals (50 individuals in total) were initially collected from the Mediterranean
434 (Elba, Italy, 42.7782° N, 10.1927° E). The slug cultures were routinely maintained essentially as described
435 by Schmitt et al. (2014). Briefly, *E. timida* were maintained at the same conditions as the cultures of
436 *Acetabularia*, their prey alga, in aerated 5-10 l plastic tanks containing 3.7 % ASW. Newly prepared ASW
437 was added to the tanks weekly to dilute contaminants and slug excrements, and the slugs were placed in
438 new tanks with fresh ASW at 3-5 week intervals. Similar to *Acetabularia* tanks, also the lids of the slug
439 tanks were locked in place. The tanks were aerated with a silicon tubes connected to air spargers (Figure

440 1E). Differing amounts of *Acetabularia* were added to the slug tanks at irregular intervals, usually once
441 every two weeks. When the adult slugs were transferred to new tanks, the old tanks with their contents
442 were not discarded but supplemented with fresh ASW media and *Acetabularia* in order to allow
443 unhatched slugs or slugs still in their veliger stage to develop into juvenile/adult slugs that are visible to
444 the eye and could be pipetted out with a 10 ml plastic Pasteur pipette. The development from
445 microscopic veligers to juvenile slugs usually took 2-3 weeks. Our method for cultivating slugs has
446 enabled us to maintain a constant slug population consisting of 500-1000 slugs with relatively little
447 labour and cost for years. It is, however, difficult to maintain the slug cultures axenic, and the slug tanks
448 do foul, if not attended to. The contaminants in our laboratory cultures have not yet been identified but,
449 based on optical inspection, seem to consist mainly of diatoms and ciliates. These organisms are likely
450 derived from the Mediterranean and have been co-cultured with the slugs throughout the years. All
451 slugs used in the experiments were always transferred into new tanks filled with fresh ASW and fed with
452 abundant *Acetabularia* for 1-2 weeks prior to the experiments, unless mentioned otherwise. Slug
453 individuals taken straight from the normal culture conditions were used for some of the measurements,
454 without special considerations on the retention status of the chloroplasts inside the slugs, i.e. the slugs
455 were not allowed to incorporate the chloroplasts overnight in the dark. The use of slugs without
456 overnight settling time is indicated in the figures.

457 Acclimating *Acetabularia* to elevated CO₂ levels was done in a closed culture cabinet (Algaetron AG230;
458 Photon Systems Instruments, Drásov, Czech Republic) by raising the CO₂ level from the ambient
459 concentration (0.04 % of air volume) to 1 % CO₂ inside the cabinet. Plastic 5 l tanks filled with
460 *Acetabularia* were placed inside the cabinet and the tank lids were slightly opened, i.e. one of the plastic
461 lid locks was not locked, to facilitate gas exchange. Newly made f/2 medium was added every second
462 day to account for evaporation (approximately 50 ml per week, estimated in a separate tank) as a
463 precaution. This can admittedly lead to salinity fluctuations, but we chose to add f/2 medium instead of
464 water, as the evaporation in our conditions was low. Incident light provided by the growth cabinet white
465 LEDs (see Figure 7 – figure supplement 1A for the spectrum) was adjusted to PPFD 40 $\mu\text{mol m}^{-2}\text{s}^{-1}$ and
466 the day-night cycle was 12/12 h. Temperature was maintained at 23 °C. The algae were always
467 acclimated for a minimum of three days to high CO₂ prior to any measurements or feeding of the slugs
468 with high-CO₂ acclimated algae.

469 The red morphotype of *Acetabularia* was induced by growing the algae at 10 °C and continuous high
470 white light (PPFD 600 $\mu\text{mol m}^{-2}\text{s}^{-1}$) for 31 days in a closed culture cabinet in ambient air (Algaetron

471 AG230; Photon Systems Instruments), essentially as described by Costa et al. (2012). While this
472 procedure was successful in producing the desired colour morphotype of *Acetabularia*, the yield was
473 very low, and most of the *Acetabularia* cells bleached during the treatment. A few cells of red
474 *Acetabularia* could be found in tanks where the cell concentration had been high enough to create a
475 light attenuating algal mat. These red *Acetabularia* cells were then collected and used for measurements
476 or fed to the slugs as indicated.

477 *E. timida* individuals that were devoid of chloroplasts, i.e. bleached, were obtained by subjecting freshly
478 fed slugs to starvation in high light (Ikea Växer PAR30 E27, 10 W; PPFD>1000 $\mu\text{mol m}^{-2}\text{s}^{-1}$; 12/12h
479 day/night) in otherwise normal growth conditions. After one week of starvation the coloration of the
480 slugs was estimated by eye, and only the palest individuals were selected for further experiments.

481 Protein analysis

482 Crude total proteins were extracted from *Acetabularia* cells grown in ambient air and high CO₂
483 conditions by cutting up approximately 4 g (wet weight) of algae with a razor blade and then grinding
484 them in 500 μl of lysis buffer (50 mM Tris-HCl pH 8, 2% SDS, 10 mM EDTA) using a 1 ml Dounce tissue
485 grinder (DWK Life Sciences, Millville, NJ, USA). The homogenate was filtered through one layer of
486 Miracloth (Calbiochem, Darmstadt, Germany). Algae used for the extractions were taken straight from
487 their respective growth conditions. All protein isolation procedures were performed at 4°C in dim light.
488 Protein concentrations from the homogenates were determined with DC™ Protein Assay (Bio-Rad,
489 Hercules, CA, USA) using BSA as a standard.

490 Aliquots containing 25 μg protein were solubilized and separated by electrophoresis on a 10 % SDS-
491 polyacrylamide gel using Next Gel solutions and buffers according to the manufacturer's instructions
492 (VWR, Radnor, PA, USA). Proteins were transferred to Immobilon-P PVDF membranes (MilliporeSigma,
493 Burlington, MA, USA). FLVs were immunodetected using an antibody raised against *C. reinhardtii* FLVB,
494 reacting with *C. reinhardtii* FLVA and FLVB (Jokel et al., 2015). Western blots were imaged using goat
495 anti-rabbit IgG (H+L) alkaline phosphatase conjugate (Life Technologies, Carlsbad, CA, USA) and CDP-star
496 Chemiluminescence Reagent (Perkin-Elmer, Waltham, MA, USA). Protein bands were quantified using
497 Fiji image processing software (Schindelin et al., 2012). Total protein extract from wild-type *C. reinhardtii*
498 strain CC406 was used as a positive control of FLVs (Jokel et al., 2015).

499 Fast kinetics of Q_A^- reoxidation, fluorescence induction (OJIP), P700 oxidation and ECS

500 Algae and slug samples were dark acclimated for 1-2 h prior to the fast kinetics measurements and all
501 fast kinetics were measured at room temperature. PSII electron transfer was blocked in certain
502 measurements, as indicated in the figures, with DCMU. For this, a 2 mM stock solution of DCMU in
503 dimethylsulfoxide was prepared and diluted to a final concentration of 10 μ M in either f/2 or ASW
504 medium, depending on whether it was administered to the algae or the slugs, respectively. DCMU was
505 only applied to samples that had been in the dark for 1 h and the dark acclimation in the presence of
506 DCMU was continued for additional 20 min. When pertinent, DCMU containing medium was applied to
507 cover the samples during the actual measurements too.

508 Anaerobic conditions were achieved by a combination of glucose oxidase (8 units/ml), glucose (6 mM)
509 and catalase (800 units/ml) in f/2 or ASW medium. Our data shows that using the above reagents and
510 concentrations in a sealed vial with stirring, nearly all oxygen was consumed from 250 ml of ASW media
511 in a matter of minutes (Figure 2 – figure supplement 1A). Similar to the DCMU treatments, anaerobic
512 conditions were initiated only after the samples had been in the dark for 1 h. In the case of *Acetabularia*,
513 the samples were placed inside a sealed 50 ml centrifuge tube filled with f/2 medium that had been pre-
514 treated with the glucose oxidase system for 10 min. The algae were then kept inside the sealed tube for
515 5 min in the dark, after which they were picked out and placed to the sample holder of the instrument in
516 question. In order to maintain oxygen concentrations as low as possible, the samples were then covered
517 with the anaerobic medium and left in the dark for additional 5 min, so that the oxygen mixed into the
518 medium during sample placement would be depleted. Before imposing anaerobic conditions to slug
519 individuals, they were swiftly decapitated with a razor blade, a procedure that has been shown not to
520 significantly affect PSII activity in the photosynthetic sea slug *Elysia viridis* during a 2 h measurement
521 period (Cruz et al., 2015). The euthanized slugs were then treated identically to the algae used in the
522 anaerobic measurements.

523 Q_A^- reoxidation kinetics after a strong single turnover (ST) flash (maximum PPFD 100 000 μ mol $m^{-2}s^{-1}$,
524 according to the manufacturer) were measured using an FL 200 fluorometer with a SuperHead optical
525 unit (Photon Systems Instruments, Drásov, Czech Republic) utilizing the software and protocol provided
526 by the manufacturer. The measurement protocol was optimized to be robust enough to allow its use in
527 measurements from both *Acetabularia* and the slugs. The parameters used in the script were as follows:
528 experiment duration - 120 s, Number of datapoints/decade - 8, First datapoint after ST flash - 150 μ s, ST
529 flash voltage – 100 %, ST flash duration – 30 μ s, measuring beam (MB) voltage – 60 %. The wavelength

530 for the ST flash and the MB was 625 nm. The option to enhance the ST flash intensity by complementing
531 it with the MB light source was not used in the measurements. Number of datapoints/decade was
532 changed to 2 for the measurements in the presence of DCMU.

533 The slugs tend to crawl around any typical cuboid 2 ml measuring cuvette if the cuvette is filled with
534 ASW, which causes disturbances to the fluorescence signal. On the other hand, if ASW is removed from
535 the cuvette, the slugs tend to stick to the bottom, placing them away from the light path of the
536 instrument. For this reason, a compromise was made between ideal optics and slug immobilization by
537 placing 3-5 slugs into a regular 1.5 ml microcentrifuge tube and then pipetting most of the ASW out of
538 the tube, leaving just enough ASW to cover the slugs. Only in the measurements in anaerobic conditions
539 were the tubes filled with oxygen depleted ASW. The tube was placed into the cuvette holder of the
540 SuperHead optical unit so that the narrow bottom of the tube with the slugs was situated in the middle
541 of the light path of the instrument and the tube was resting on its top appendices. The tube caps were
542 left open for the measurements without any inhibitors and in the presence of DCMU, unlike the
543 anaerobic measurements where the caps were closed. In the context of Q_A^- reoxidation data from the
544 slugs, one biological replicate refers to one measurement from 3-5 slugs inside the same tube in this
545 study. Completely new slugs were used for each biological replicate. In order to facilitate comparison,
546 Q_A^- reoxidation from the algae was also measured using 1.5 ml microcentrifuge tubes, but due to the
547 sessile nature of the algae there was no need to remove the f/2 media from the tubes. For each
548 biological replicate representing the algae in the Q_A^- reoxidation data sets, approximately 5-10 cells were
549 placed inside each of the tubes.

550 The polyphasic fluorescence rise kinetics (OJIP curves) were measured with AquaPen-P AP 110-P
551 fluorometer (Photon Systems Instruments) that has an inbuilt LED emitter providing 455 nm light for the
552 measurements. The fluorometer was mounted on a stand and all measurements were done by placing a
553 Petri dish with the sample on it on a matte black surface and positioning the sample directly under the
554 probe head of the fluorometer. The intensity of the 2 s multiple turnover (MT) saturating pulse used for
555 the measurements was optimized separately for measurements from single slug individuals
556 (representing one biological replicate) and 1-2 cells/strands of algae (representing one biological
557 replicate) placed under the probe of the instrument.

558 The final MT pulse intensity setting of the instrument was 70 % (100 % being equal to PPFD 3000 μmol
559 $\text{m}^{-2}\text{s}^{-1}$ according to the manufacturer's specifications) for the slugs and 50 % for *Acetabularia*. OJIP
560 curves were measured from samples that had been covered in their respective treatment media, which

561 presented a concern with regard to the anaerobic measurements, as the samples were not in a closed
562 environment and oxygen diffusion into the sample could not be prevented. The data in Figure 2 – figure
563 supplement 1B shows that diffusion is largely negated during the additional 5 min dark period even in an
564 open setup. The conditions during these OJIP measurements will be referred to as anaerobic although
565 some diffusion of oxygen to the samples occurred.

566 Fast kinetics of P700 oxidation during a 780 ms MT pulse were measured with Dual-PAM 100 (Heinz
567 Walz GmbH, Effeltrich, Germany) equipped with the linear positioning system stand 3010-DUAL/B
568 designed for plant leaves and DUAL-E measuring head that detects absorbance changes at 830 nm
569 (using 870 nm as a reference wavelength). The absorbance changes are not caused entirely by P700
570 redox state, as the contribution of other components of the electron transfer chain, plastocyanin and
571 ferredoxin, cannot be distinguished from the P700 signal at this wavelength region (Klughammer and
572 Schreiber, 2016). P700 measurements were carried out essentially as described by (Shimakava et al.,
573 2019), with slight modifications. We built a custom sample holder frame that can be sealed from the top
574 and bottom with two microscope slide cover glasses by sliding the cover glasses into the frame. The
575 frame of this sample holder was wide enough so that the soft stoppers of the Dual-PAM detector unit's
576 light guide could rest on it without disturbing the sample even when the top cover glass was not in
577 place. A 3D-printable file for the sample holder is available at
578 <https://seafiler.utu.fi/d/2bf6b91e85644daeb064/>.

579 The 635 nm light provided by the LED array of Dual-PAM was used for the MT pulse (780 ms, PPFD
580 $10000 \mu\text{mol m}^{-2}\text{s}^{-1}$) in the P700⁺ measurements. Fluorescence was not measured during the MT pulse, as
581 the MB used for fluorescence seemed to disturb the P700⁺ signal from the slugs. The drift of the signal
582 made attempts to estimate the maximum oxidation level of P700 according to the standard protocol
583 described by Schreiber and Klughammer (2008a) impossible with the slugs. Measurements from the
584 algae would not have required any special considerations due to a stronger signal, but the algae were
585 nevertheless measured identically to the slugs for the sake of comparability. The measuring light
586 intensity used for detecting the P700 absorbance changes had to be adjusted individually for each
587 sample. All P700⁺ kinetics were measured from individual slugs (i.e one slug represents one biological
588 replicate), as pooling multiple slugs together for a single measurement did not noticeably enhance the
589 signal.

590 Due to the delicate nature of the P700⁺ signal, all slugs used for these measurements had to be
591 decapitated with a razor blade before the measurements. It is important to note that obtaining a single,

592 meaningful fast kinetics curve of P700 oxidation requires sacrificing a lot of slug individuals. In this study
593 a minimum of 10 individuals were used to construct each curve, because in approximately 30-50 % of
594 the measurements the signal was simply too noisy and drifting to contain any meaningful information.

595 The P700⁺ measurements were carried out similarly to the OJIP measurements, with three main
596 differences. First, the number of algae cells per measurement (representing one biological replicate) was
597 higher, usually 5-10 cells/strands forming an almost solid green area between the light guides of Dual-
598 PAM inside the sample holder. Secondly, the anaerobic measurements were carried out in a sealed
599 system, achieved by closing the sample holder with both cover glasses after filling it with anaerobic
600 medium. Measurements from all other treatments were carried out in open sample holders. The third
601 difference was that for some of the experiments a second MT pulse was fired after a 10 s dark period
602 following the first MT pulse. This procedure is referred to as “second pulse P700 redox kinetics protocol”
603 in the main text.

604 Electrochromic shift (ECS, or P515) during a MT pulse (780 ms, 635 nm, PPFD 10000 $\mu\text{mol m}^{-2}\text{s}^{-1}$) was
605 measured with P515 module of Dual-PAM 100 using the dual beam 550-515 transmittance difference
606 signal (actual wavelengths used were 550 and 520 nm) (Schreiber and Klughammer, 2008b; Klughammer
607 et al., 2013). ECS from *Acetabularia* was measured using the exact same setup as with the P700
608 measurements, but ECS from the slug *E. timida* could only be measured using the pinhole accessory of
609 Dual-PAM 100. Shortly, a pinhole plug was placed on the optical rod of the P515 detector and 3-5
610 decapitated slug individuals (representing one biological replicate) were placed into the hole of the plug,
611 covering the optical path. After placing a sample between the optical rods of the P515 module, the ECS
612 signal was calibrated and the MB was turned off to decrease the actinic effect caused by the MB. MB
613 was turned back on again right before measuring the ECS kinetics during a MT pulse. The intensity of the
614 MB was adjusted for each sample separately.

615 The P700 oxidation and ECS data from *E. timida* and *Acetabularia* were slope corrected, when needed,
616 using the baseline subtraction tool of Origin 2016 v.9.3 (OriginLab Corporation, Northampton, MA, USA)
617 to account for signal drift. All biological replicates used to construct the fast kinetics data figures (Q_A^-
618 reoxidation, OJIP, P700 oxidation and ECS) were normalized individually as indicated in the main text
619 figures, and the normalized data were averaged to facilitate comparison between the samples.

620 Maximum quantum yield of PSII and rapid light response curves

621 Maximum quantum yield of PSII photochemistry (F_V/F_M) was routinely measured from slug individuals
622 using PAM-2000 fluorometer (Heinz Walz GmbH) after minimum of 20 min darkness. The measurements
623 were carried out by placing a dark acclimated slug on to the side of an empty Petri dish and then
624 pipetting all ASW media out, leaving the slug relatively immobile for the time required for the
625 measurement. The light guide of PAM-2000 was hand-held at a $\sim 45^\circ$ angle respective to the slug, using
626 the side and bottom of the Petri dish as support, and a saturating pulse was fired. PAM-2000 settings
627 used for F_V/F_M measurements from the slugs were as follows: MB intensity 10 (maximum), MB
628 frequency 0.6 kHz, high MB frequency 20 kHz (automatically on during actinic light illumination), MT
629 pulse intensity 10 (maximum, PPFD $>10\,000\ \mu\text{mol m}^{-2}\text{s}^{-1}$), MT pulse duration 0.8 s.

630 Measuring rapid light curves (RLCs) requires total immobilization of the slugs, a topic that has been
631 thoroughly discussed by Cruz et al. (2012). Instead of using the anaesthetic immobilization technique
632 described by Cruz et al. (2012), we tested yet another immobilization method to broaden the toolkit
633 available for studying photosynthesis in Sacoglossan sea slugs. Alginate is a porous, biologically inert and
634 transparent polymer that is widely used for fixing unicellular algae and cyanobacteria to create uniform
635 and easy to handle biofilms or beads in e.g. biofuel research (Kosourov and Seibert, 2009; Antal et al.,
636 2014). For the fixation of the slugs, an individual slug (representing one biological replicate) was placed
637 on a Petri dish and a small drop of 1 % alginate (m/v in H_2O) was pipetted on top of the slug, covering
638 the slug entirely. Next, roughly the same volume of 0.5 mM CaCl_2 was distributed evenly to the alginate
639 drop to allow the Ca^{2+} ions to rapidly polymerize the alginate. The polymerization was allowed to
640 continue for 10-30 s until the alginate had visibly solidified. All leftover CaCl_2 was removed with a tissue,
641 and the slug fixed inside the alginate drop was placed under the fixed light guide of PAM-2000, in direct
642 contact and in a 90° angle, for the measurement. After the measurement was over, the alginate drop
643 was covered with abundant 1M Na-EDTA to rapidly chelate the Ca^{2+} ions and depolymerize the alginate.
644 Once the slug was visibly free of alginate, it was immediately transferred to fresh ASW for rinsing with a
645 Pasteur pipette. The slugs usually recovered full movement, defined as climbing the walls of the
646 container, in 10-20 min. The slugs were placed into a new tank for breeding purposes once motility had
647 been restored. We also tested the effect of alginate fixation on F_V/F_M during a 10 min time period, a
648 typical length for RLC measurements, and no effect was noticeable (Figure 5 – figure supplement 1). All
649 RLCs from algae were measured from 5-10 cells/measurement (representing one biological replicate),
650 using otherwise the same setup as with the slugs, except that alginate fixation was not applied. The

651 basic settings for RLC measurements were the same as with F_v/F_M measurements, except for the MB
652 intensity, which was adjusted to setting 5 with the algae to avoid oversaturation of the signal. Each light
653 step lasted 90 s and the PPFs that were used are shown in the figures. rETR was calculated as
654 $0.42 \cdot Y(II) \cdot \text{PPFD}$, where 0.42 represents the fraction of incident photons absorbed by PSII, based on
655 higher plant leaf assumptions, and $Y(II)$ represents effective quantum yield of PSII photochemistry under
656 illumination. NPQ was calculated as $F_M/F_M' - 1$, where F_M' represent maximum chlorophyll fluorescence of
657 illuminated samples. See Kalaji et al. (2014) for detailed descriptions of rETR and NPQ.

658 Feeding experiments

659 In order to ensure that the slugs incorporate only specifically acclimated chloroplasts inside their own
660 cells, the first feeding experiment was done with slug individuals that had been kept away from their
661 food for four weeks in 5 l tanks filled with fresh ASW medium in their normal culture conditions. The
662 coloration of the slugs was pale after the starvation period, indicating a decrease in the chloroplast
663 content within the slugs. Altogether 107 starved slug individuals were selected for the feeding
664 experiments and divided to two tanks filled with abundant *Acetabularia* in f/2 culture medium, one tank
665 containing high-CO₂ acclimated algae (54 slugs) and the other one algae grown in ambient air (53 slugs).
666 The tanks with the slugs and algae in them were put to their respective growth conditions for 4 days to
667 allow the slugs to incorporate new chloroplasts inside their cells. The tanks were not aerated during the
668 feeding, but the tank lids were unlocked for both feeding groups. The elevated CO₂ level in the closed
669 culture cabinet posed a problem, as it noticeably affected the slug behaviour by making them sessile in
670 comparison to normal growth conditions, probably due to increased replacement of O₂ by CO₂. Because
671 of this, the slugs selected for feeding on the high-CO₂ acclimated algae were fed in cycles where the
672 tanks were in the closed CO₂ cabinet for most of the time during the daylight hours, but taken out every
673 few hours and mixed with ambient air by stirring and kept in the ambient-air conditions for 1-2 hours
674 before taking the tanks back to the high-CO₂ cabinet. The tanks were always left inside the closed
675 cabinets for the nights in order to inflict minimal changes to the acclimation state of the algae. After 4
676 days of feeding, 50 slug individuals of similar size and coloration were selected from both feeding groups
677 and distributed into 2 new 5 l tanks/feeding group, filled with approximately 2 l of 3.7 % ASW medium
678 and containing no algae. All slugs (25+25 ambient-air slugs, 25+25 high-CO₂ slugs) were moved to
679 ambient-air growth conditions and kept in the dark overnight in order to allow maximal incorporation of
680 the chloroplasts before starting the starvation experiment in steady-light conditions.

681 For the second feeding experiment the four-week pre-starvation period of the slugs was discarded to
682 see whether the differences in photosynthetic parameters between the two feeding groups could be
683 inflicted just by allowing the slugs to replace their old kleptoplasts with the specific chloroplasts fed to
684 them. We selected 100 slugs from normal growth conditions and divided them once again into two
685 tanks containing *f/2* culture medium and *Acetabularia* that had been acclimated to ambient air (50
686 slugs) or high CO₂ (50 slugs). The slugs were allowed to feed for 6 days, but otherwise the feeding
687 protocol was identical to the one used in the first feeding experiment. After the sixth day of feeding, 45
688 slug individuals of similar size and coloration were selected from both feeding groups and divided to 2
689 new 5 l tanks (20+25 ambient-air slugs, 20+25 1 % CO₂ slugs) filled with approx. 2 l of ASW and kept
690 overnight in the dark before starting the starvation experiment in fluctuating light.

691 A third feeding experiment was conducted in order to create the red morphotype of *E. timida* (González-
692 Wangüemert et al., 2006; Costa et al., 2012). Slug individuals from normal growth conditions were
693 selected and placed in Petri dishes filled with *f/2* culture medium and abundant red *Acetabularia*. The
694 slugs were allowed to eat the algae for 2 days in the normal culture conditions of the slugs prior to the
695 measurements. Three Petri dishes were filled with just the red form *Acetabularia* in *f/2* culture medium
696 in exactly the same conditions, and these algae were used for measurements regarding the red
697 morphotypes of *Acetabularia* and *E. timida*.

698 Starvation experiments

699 Two different starvation experiments were carried out with ambient-air slugs and high-CO₂ slugs. In the
700 first one the slugs from the first feeding experiment were starved in steady-light conditions, where the
701 only changes in the incident light were due to the day/night light cycle (12/12 h). Here, all four tanks
702 (25+25 ambient-air slugs, 25+25 high-CO₂ slugs) were placed under white LED lights (Växer PAR30 E27,
703 10 W; Ikea, Delft, The Netherlands; see Figure 7 – figure supplement 1B for the spectrum) adjusted to
704 PPFD 40 $\mu\text{mol m}^{-2}\text{s}^{-1}$. Temperature was maintained at 23 °C and the tanks were not aerated during the
705 starvation experiment apart from the passive gas flux that was facilitated by the unlocked lids of the
706 tanks. Fresh ASW medium (approximately 500 ml) was added to the tanks every second day and the
707 slugs were placed into new tanks with fresh ASW 1-2 times a week throughout the entire starvation
708 period of 46 days. The day following the overnight dark period that the slugs were subjected to after the
709 feeding experiment was noted as day 0 in the starvation experiments. F_V/F_M during starvation was
710 measured from individual slugs (representing one biological replicate) as indicated in the main text
711 figures. Sampling caused losses to the slug populations on days 0, 5 and 15, when 10 slug

712 individuals/group were selected for P700 oxidation kinetics measurements. Unfortunately, the P700⁺
713 signals after 15 days in starvation were too weak and noisy for any meaningful interpretations. Before
714 day 25, starvation induced mortality of both groups was 0. After that the ambient-air slug population
715 suffered losses on days 27 (1 slug), 35 (2 slugs), 45 (5 slugs), 46 (1 slug) altogether 9 slugs. For the high-
716 CO₂ slug population the losses were as follows: day 27 (1 slug), 29 (1 slug), 31 (1 slug), 45 (8 slugs) and 46
717 (1 slug), 12 slugs in total. Lengths of the slugs were estimated from images taken at set intervals
718 essentially as described by Christa et al. (2018). Images were taken with a cropped sensor DSLR camera
719 equipped with a macro lens (Canon EOS 7D MKII + Canon EF-S 60mm f/2.8 Macro lens; Canon Inc.,
720 Tokyo, Japan) and the body length of each slug individual was estimated using the image analysis
721 software Fiji (Schindelin et al., 2012). The slugs from both feeding groups were pooled into one
722 tank/group after day 25 in starvation.

723 The second starvation experiment was carried out using ambient-air slugs and high-CO₂ slugs from the
724 second feeding experiment. The four tanks from both feeding groups (20+25 ambient-air slugs, 20+25
725 high-CO₂ slugs) were placed under a fluctuating light regime. The day/night cycle was maintained at
726 12/12 h, but during the daylight hours the background illumination (PPFD 40 $\mu\text{mol m}^{-2}\text{s}^{-1}$) was
727 supplemented with a 10 s pulse of high light (PPFD 1500 $\mu\text{mol m}^{-2}\text{s}^{-1}$) every 10 minutes. Both the
728 background illumination and the high-light pulses originated from a programmable Heliospectra L4A
729 greenhouse lamp (model 001.010; Heliospectra, Göteborg, Sweden; see Figure 7 – figure supplement 1B
730 for the irradiance spectra). All other conditions and procedures were identical to the ones used in the
731 first starvation experiment. F_v/F_m during starvation was measured as indicated in the main text figures.
732 Sampling caused losses to the slug populations on days 0 and 6, when 10 slugs/group were selected for
733 P700 redox kinetics measurements, and on day 10, when 5 slugs/group were selected for RLC
734 measurements. No images were taken during the starvation experiment in fluctuating light. The slugs
735 were pooled into one tank/feeding group after 25 days in starvation. Chlorophyll was extracted from the
736 slugs with N,N-dimethylformamide and chlorophyll *a/b* was estimated spectrophotometrically according
737 to Porra et al. (1989).

738 Acknowledgments

739 This study was funded by Academy of Finland (grants 307335 and 333421). V.H. was supported by
740 Finnish Cultural Foundation, Väisälä Fund and University of Turku Graduate School (UTUGS). Sven. B.
741 Gould and his research group are acknowledged for the invaluable help in establishing laboratory

742 cultures of both *E. timida* and *Acetabularia*, and Taras Antal for help with fluorescence induction
 743 measurements. We are grateful to associate professor Yagut Allahverdiyeva-Rinne for the FLVB
 744 antibody, and Martina Jokel-Toivanen is thanked for advice concerning its use.

745 Competing interests

746 The authors declare no competing interests.

747 References

- 748 1. Alboresi A, Storti M, Cendron L, Morosinotto T (2019) Role and regulation of class-C flavodiiron
 749 proteins in photosynthetic organisms. *Biochem. J.* 476: 2487–2498.
 750 <https://doi.org/10.1042/BCJ20180648>
- 751 2. Allahverdiyeva Y, Isojärvi J, Zhang O, Aro EM (2015) Cyanobacterial Oxygenic Photosynthesis is
 752 Protected by Flavodiiron Proteins. *Life* 5: 716-743. <https://doi.org/10.3390/life5010716>
- 753 3. Antal TK, Matorin DN, Kukarskikh GP, Lambreva MD, Tyystjärvi E, Krendeleva TE, Tsygankov AA,
 754 Rubin AB (2014) Pathways of hydrogen photoproduction by immobilized *Chlamydomonas*
 755 *reinhardtii* cells deprived of sulfur. *Int. J. Hydrog. Energy* 39: 18194–1820.
 756 <https://doi.org/10.1016/j.ijhydene.2014.08.135>
- 757 4. Bulychev AA, Cherkashin AA, Muronets EM, Elanskaya IV (2018) Photoinduction of electron
 758 transport on the acceptor side of PSI in *Synechocystis* PCC 6803 mutant deficient in flavodiiron
 759 proteins Flv1 and Flv3. *Biochim. Biophys. Acta* 1859: 1086-1095.
 760 <https://doi.org/10.1016/j.bbabi.2018.06.012>
- 761 5. Cartaxana P, Trampe E, Kühl M, Cruz S (2017) Kleptoplast photosynthesis is nutritionally relevant
 762 in the sea slug *Elysia viridis*. *Sci. Rep.* 7: 7714. <https://doi.org/10.1038/s41598-017-08002-0>
- 763 6. Cartaxana P, Morelli L, Jesus B, Calado G, Calado R, Cruz S (2019) The photon menace:
 764 kleptoplast protection in the photosynthetic sea slug *Elysia timida*. *J. Exp. Biol.* 222: jeb202580.
 765 <https://doi.org/10.1242/jeb.202580>
- 766 7. Christa G, Pütz L, Sickinger C, Melo Clavijo J, ELaetz EMJ, Greve C, Serôdio J (2018)
 767 Photoprotective non-photochemical quenching does not prevent kleptoplasts from net
 768 photoinactivation. *Front. Ecol. Evol.* 6:121. <https://doi.org/10.3389/fevo.2018.00121>
- 769 8. Cooper JJ, Mandoli DF (1999) Physiological factors that aid differentiation of zygotes and early
 770 juveniles of *Acetabularia acetabulum* (Chlorophyta). *J. Phycol.* 35: 143-151.
 771 <https://doi.org/10.1046/j.1529-8817.1999.3510143.x>

- 772 9. Costa J, Giménez-Casalduero F, Melo RA, Jesus B (2012) Colour morphotypes of *Elysia timida*
773 (Sacoglossa, Gastropoda) are determined by light acclimation in food algae. *Aquat. Biol.* 17: 81-
774 89. <https://doi.org/10.3354/ab00446>
- 775 10. Cruz S, Dionísio G, Rosa R, Calado R, Serôdio J (2012) Anesthetizing solar-powered sea slugs for
776 photobiological studies. *Biol. Bull.* 223: 328–336. <https://doi.org/10.1086/BBLv223n3p328>
- 777 11. Cruz S, Calado R, Serôdio J, Cartaxana P (2013) Crawling leaves: photosynthesis in sacoglossan
778 sea slugs. *J. Exp. Bot.* 64: 3999–4009. <https://doi.org/10.1093/jxb/ert197>
- 779 12. Cruz S, Cartaxana P, Newcomer R, Dionísio G, Calado R, Serôdio J, Pelletreau KN, Rumpho ME
780 (2015) Photoprotection in sequestered plastids of sea slugs and respective algal sources. *Sci.*
781 *Rep.* 5 : 7904. <https://doi.org/10.1038/srep07904>
- 782 13. de Vries J, Habicht J, Woehle C, Huang C, Christa G, Wägele H, Nickelsen J, Martin WF, Gould SB
783 (2013) Is ftsH the key to plastid longevity in sacoglossan slugs? *Genome Biol. Evol.* 5: 2540-8.
784 <https://doi.org/10.1093/gbe/evt205>
- 785 14. de Vries J, Christa G, Gould SB (2014) Plastid survival in the cytosol of animal cells. *Trends Plant*
786 *Sci.* 19: 347-350. <https://doi.org/10.1016/j.tplants.2014.03.010>
- 787 15. de Vries J, Woehle C, Christa G, Wägele H, Tielens AGM, Jahns P, Gould SB (2015) Comparison of
788 sister species identifies factors underpinning plastid compatibility in green sea slugs. *Proc. R.*
789 *Soc. B.* 282: 20142519. <https://doi.org/10.1098/rspb.2014.2519>
- 790 16. de Wijn R, van Gorkom HJ (2001) Kinetics of electron transfer from Q_A to Q_B in Photosystem II.
791 *Biochemistry* 40: 11912-11922. <https://doi.org/10.1021/bi010852r>
- 792 17. Deák Z, Sass L, Kiss É, Vass I (2014) Characterization of wave phenomena in the relaxation of
793 flash-induced chlorophyll fluorescence yield in cyanobacteria. *Biochim. Biophys. Acta* 1837:
794 1522-1532. <https://doi.org/10.1016/j.bbabi.2014.01.003>
- 795 18. Ermakova M, Huokko T, Richaud P, Bersanini L, Howe CJ, Lea-Smith DJ, Peltier G, Allahverdiyeva
796 Y (2016) Distinguishing the roles of thylakoid respiratory terminal oxidases in the
797 cyanobacterium *Synechocystis* sp. PCC 6803. *Plant Physiol.* 171: 1307–1319.
798 <https://doi.org/10.1104/pp.16.00479>
- 799 19. Gerotto C, Alboresi A, Meneghesso A, Jokel M, Suorsa M, Aro EM, Morosinotto T (2016)
800 Flavodiiron proteins as safety valve for electrons in *Physcomitrella patens*. *Proc. Natl. Acad. Sci.*
801 *USA* 113: 12322–12327. <https://doi.org/10.1073/pnas.1606685113>
- 802 20. González-Wangüemert M, Francisca Giménez-Casalduero F, Perez-Ruzafa A (2006) Genetic
803 differentiation of *Elysia timida* (Risso, 1818) populations in the Southwest Mediterranean and

- 804 Mar Menor coastal lagoon. *Biochem. Syst. Ecol.* 34:514-527.
805 <https://doi.org/10.1016/j.bse.2005.12.009>
- 806 21. Havurinne V, Mattila H, Antinluoma M, Tyystjärvi E (2018) Unresolved quenching mechanisms of
807 chlorophyll fluorescence may invalidate multiple turnover saturating pulse analyses of
808 photosynthetic electron transfer in microalgae. *Physiol. Plant.* 166: 365–379.
809 <https://doi.org/10.1111/ppl.12829>
- 810 22. Hunt BE, Mandoli DF (1992) Axenic cultures of *Acetabularia* (Chlorophyta): A decontamination
811 protocol with potential application to other algae. *J. Phycol.* 28: 407-414.
812 <https://doi.org/10.1111/j.0022-3646.1992.00407.x>
- 813 23. Ilík P, Pavlovič A, Kouřil R, Alboresi A, Morosinotto T, Allahverdiyeva Y, Aro EM, Yamamoto H,
814 Shikanai T (2017) Alternative electron transport mediated by flavodiiron proteins is operational
815 in organisms from cyanobacteria up to gymnosperms. *New Phytol.* 214: 967–972.
816 <https://doi.org/10.1111/nph.14536>
- 817 24. Järvi S, Suorsa M, Aro EM (2015) Photosystem II repair in plant chloroplasts - Regulation,
818 assisting proteins and shared components with photosystem II biogenesis. *Biochim. Biophys.*
819 *Acta* 1847: 900-9. <https://doi.org/10.1016/j.bbabi.2015.01.006>
- 820 25. Jokel M, Kosourov S, Battchikova N, Tsygankov AA, Aro EM, Allahverdiyeva Y (2015)
821 *Chlamydomonas* flavodiiron proteins facilitate acclimation to anoxia during sulfur deprivation.
822 *Plant Cell Physiol.* 56: 1598-1607. <https://doi.org/10.1093/pcp/pcv085>
- 823 26. Jokel M, Johnson X, Peltier G, Aro EM, Allahverdiyeva Y (2018) Hunting the main player enabling
824 *Chlamydomonas reinhardtii* growth under fluctuating light. *Plant J.* 94: 822–835.
825 <https://doi.org/10.1111/tpj.13897>
- 826 27. Kalaji HM, Schansker G, Ladle RJ, Goltsev V, Bosa K, Allahverdiyev SI, Brestic M, Bussotti F,
827 Calatayud A, Dąbrowski P, Elsheery NI, Ferroni L, Guidi L, Hogewoning SW, Jajoo A, Misra AN,
828 Nebauer SG, Pancaldi S, Penella C, Poli DB, Pollastrini M, Romanowska-Duda ZB, Rutkowska B,
829 Serôdio J, Suresh K, Szulc W, Tambussi E, Yannicari M, Zivcak M (2014) Frequently asked
830 questions about *in vivo* chlorophyll fluorescence: practical issues. *Photosynth. Res.* 122: 121–
831 158. <https://doi.org/10.1007/s11120-014-0024-6>
- 832 28. Khorobrykh S, Havurinne V, Mattila H, Tyystjärvi E (2020) Oxygen and ROS in photosynthesis.
833 *Plants* 9: 91. <https://doi.org/10.3390/plants9010091>

- 834 29. Klughammer C, Siebke K, Schreiber U (2013) Continuous ECS-indicated recording of the proton-
835 motive charge flux in leaves. *Photosynth. Res.* 117: 471–487. [https://doi.org/10.1007/s11120-](https://doi.org/10.1007/s11120-013-9884-4)
836 013-9884-4
- 837 30. Klughammer C, Schreiber U (2016) Deconvolution of ferredoxin, plastocyanin, and P700
838 transmittance changes in intact leaves with a new type of kinetic LED array spectrophotometer.
839 *Photosynth. Res.* 128: 195-214. <https://doi.org/10.1007/s11120-016-0219-0>
- 840 31. Kodru S, Malavath T, Devadasu E, Nellaepalli S, Stirbet A, Subramanyam R, Govindjee (2015) The
841 slow S to M rise of chlorophyll *a* fluorescence reflects transition from state 2 to state 1 in the
842 green alga *Chlamydomonas reinhardtii*. *Photosynth. Res.* 125:219-31.
843 <https://doi.org/10.1007/s11120-015-0084-2>
- 844 32. Kosourov SN, Seibert M (2009) Hydrogen photoproduction by nutrient-deprived
845 *Chlamydomonas reinhardtii* cells immobilized within thin alginate films under aerobic and
846 anaerobic conditions. *Biotechnol. Bioeng.* 102: 50-8. <https://doi.org/10.1002/bit.22050>
- 847 33. Kramer DM, Di Marco G, Loreto F (1995) Contribution of plastoquinone quenching to saturation
848 pulse-induced rise of chlorophyll fluorescence in leaves In: Mathis P (Ed.) *Photosynthesis: From*
849 *Light to Biosphere*, Vol. 1, pp 147-150. Kluwer Academic Publishers, Dordrecht, The Netherlands.
- 850 34. Krishna PS, Morello G, Mamedov F (2019) Characterization of the transient fluorescence wave
851 phenomenon that occurs during H₂ production in *Chlamydomonas reinhardtii*. *J. Exp. Bot.* 70:
852 6321–6336. <https://doi.org/10.1093/jxb/erz380>
- 853 35. Magyar M, Sipka G, Kovács L, Ughy B, Zhu Q, Han G, Špunda V, Lambrev PH, Shen J, Garab G
854 (2018) Rate-limiting steps in the dark-to-light transition of Photosystem II - revealed by
855 chlorophyll-a fluorescence induction. *Sci. Rep.* 8: 2755. [https://doi.org/10.1038/s41598-018-](https://doi.org/10.1038/s41598-018-21195-2)
856 21195-2
- 857 36. Matsubara S, Chow WS (2004) Populations of photoinactivated photosystem II reaction centers
858 characterized by chlorophyll a fluorescence lifetime *in vivo*. *Proc. Natl. Acad. Sci. USA* 101:
859 18234-18239. <https://doi.org/10.1073/pnas.0403857102>
- 860 37. Mehler AH (1951) Studies on reactivity of illuminated chloroplasts. Mechanism of the reduction
861 of oxygen and other Hill reagents. *Arch. Biochem. Biophys.* 33: 65–77.
862 [https://doi.org/10.1016/0003-9861\(51\)90082-3](https://doi.org/10.1016/0003-9861(51)90082-3)
- 863 38. Müller P, Li XP, Niyogi KK (2001) Non-Photochemical Quenching. A Response to Excess Light
864 Energy. *Plant Physiol.* 125: 1558–1566. <https://doi.org/10.1104/pp.125.4.1558>

- 865 39. Oja V, Eichelmann H, Laisk A (2011) Oxygen evolution from single- and multiple-turnover light
866 pulses: temporal kinetics of electron transport through PSII in sunflower leaves. *Photosynth. Res.*
867 110: 99-109. <https://doi.org/10.1007/s11120-011-9702-9>
- 868 40. Osmond B, Chow WS, Wyber R, Zavafer A, Keller B, Pogson BJ, Robinson SA (2017) Relative
869 functional and optical absorption cross-sections of PSII and other photosynthetic parameters
870 monitored in situ, at a distance with a time resolution of a few seconds, using a prototype light
871 induced fluorescence transient (LIFT) device. *Funct. Plant. Biol.* 44: 985-1006.
872 <https://doi.org/10.1071/FP17024>
- 873 41. Papageorgiou GC, Govindjee (2014) The non-photochemical quenching of the electronically
874 excited state of chlorophyll *a* in plants: Definitions, timelines, viewpoints, open questions. In:
875 Demmig-Adams B, Garab G, Adams WIII, Govindjee (Eds.) Non-photochemical quenching and
876 energy dissipation in plants, algae and cyanobacteria. *Advances in Photosynthesis and*
877 *Respiration*, Vol. 40, pp 1-44. Springer, Dordrecht, The Netherlands.
- 878 42. Porra RJ, Thompson WA, Kriedemann PE (1989) Determination of accurate extinction
879 coefficients and simultaneous equations for assaying chlorophyll *a* and *b* with four different
880 solvents: verification of the concentration of chlorophyll by atomic absorption spectroscopy.
881 *Biochim. Biophys. Acta* 975: 384-394. [https://doi.org/10.1016/S0005-2728\(89\)80347-0](https://doi.org/10.1016/S0005-2728(89)80347-0)
- 882 43. Rauch C, Jahns P, Tielens AGM, Gould SB, Martin WF (2017) On being the right size as an animal
883 with plastids. *Front. Plant Sci.* 8: 1402. <https://doi.org/10.3389/fpls.2017.01402>
- 884 44. Ruban AV, Horton P (1999) The xanthophyll cycle modulates the kinetics of nonphotochemical
885 energy dissipation in isolated light-harvesting complexes, intact chloroplasts, and leaves of
886 spinach. *Plant Physiol.* 119: 531-542. <https://doi.org/10.1104/pp.119.2.531>
- 887 45. Rumpho ME, Summer EJ, Manhart JR (2000) Solar-Powered Sea Slugs. Mollusc/Algal Chloroplast
888 Symbiosis. *Plant Physiol.* 123: 29-38. <https://doi.org/10.1104/pp.123.1.29>
- 889 46. Rumpho ME, Pelletreau KN, Moustafa A, Bhattacharya D (2011) The making of a photosynthetic
890 animal. *J. Exp. Biol.* 214: 303-311. <https://doi.org/10.1242/jeb.046540>
- 891 47. Santana-Sanchez A, Solymosi D, Mustila H, Bersanini L, Aro EM, Allahverdiyeva Y (2019)
892 Flavodiiron proteins 1–to-4 function in versatile combinations in O₂ photoreduction in
893 cyanobacteria. *eLife* 8: e45766. <https://doi.org/10.7554/eLife.45766>
- 894 48. Schansker G, Tóth SZ, Holzwarth AR, Garab G (2014) Chlorophyll *a* fluorescence: beyond the
895 limits of the Q_A model. *Photosynth Res.* 120: 43–58. <https://doi.org/10.1007/s11120-013-9806-5>

- 896 49. Schindelin J, Arganda-Carreras I, Frise E, Kaynig V, Longair M, Pietzsch T, Preibisch S, Rueden C,
897 Saalfeld S, Schmid B, Tinevez JY, White DJ, Hartenstein V, Eliceiri K, Tomancak P, Cardona A
898 (2012) Fiji: an open-source platform for biological-image analysis. *Nat. Methods* 9: 676–682.
899 <https://doi.org/10.1038/nmeth.2019>
- 900 50. Schmitt V, Händeler K, Gunkel S, Escande ML, Menzel D, Gould SB, Martin WF, Wägele H (2014)
901 Chloroplast incorporation and long-term photosynthetic performance through the life cycle in
902 laboratory cultures of *Elysia timida* (Sacoglossa, Heterobranchia). *Front. Zool.* 11: 5.
903 <https://doi.org/10.1186/1742-9994-11-5>
- 904 51. Schreiber U, Klughammer C (2008a) Saturation pulse method for assessment of energy
905 conversion in PSI. *PAM Appl. Notes* 1: 11-14.
- 906 52. Schreiber U, Klughammer C (2008b) New accessory for the DUAL-PAM-100: The P515/535
907 module and examples of its application. *PAM Appl. Notes* 1: 1-10.
- 908 53. Schreiber U, Klughammer C, Schansker G (2019) Rapidly reversible chlorophyll fluorescence
909 quenching induced by pulses of supersaturating light *in vivo*. *Photosynth. Res.* 142: 35-50.
910 <https://doi.org/10.1007/s11120-019-00644-7>
- 911 54. Serôdio J, Cruz S, Cartaxana P, Calado R (2014) Photophysiology of kleptoplasts: photosynthetic
912 use of light by chloroplasts living in animal cells. *Philos. Trans. R. Soc. Lond. B. Biol. Sci.* 369:
913 20130242. <https://doi.org/10.1098/rstb.2013.0242>
- 914 55. Shimakawa G, Murakami A, Niwa K, Matsuda Y, Wada A, Miyake C (2019) Comparative analysis
915 of strategies to prepare electron sinks in aquatic photoautotrophs. *Photosynth. Res.* 139: 401-
916 411. <https://doi.org/10.1007/s11120-018-0522-z>
- 917 56. Stirbet A, Govindjee (2012) Chlorophyll a fluorescence induction: a personal perspective of the
918 thermal phase, the J-I-P rise. *Photosynth. Res.* 113: 15-61. <https://doi.org/10.1007/s11120-012-9754-5>
- 920 57. Strasser RJ, Srivastava A, Govindjee (1995) Polyphasic chlorophyll a fluorescence transient in
921 plants and cyanobacteria. *Photochem. Photobiol.* 61: 32–42. <https://doi.org/10.1111/j.1751-1097.1995.tb09240.x>
- 923 58. Strasser RJ, Tsimilli-Michael M, Srivastava A (2004) Analysis of the chlorophyll a fluorescence
924 transient. In: Papageorgiou GC, Govindjee (Eds.) Chlorophyll a Fluorescence: A Signature of
925 Photosynthesis. *Advances in Photosynthesis and Respiration*, Vol. 19, pp 321-362. Springer,
926 Dordrecht, The Netherlands.

- 927 59. Suggett DJ, Oxborough K, Baker NR, Macintyre HL, Kana TM, Geider RJ (2003) Fast repetition
928 rate and pulse amplitude modulation chlorophyll *a* fluorescence measurements for assessment
929 of photosynthetic electron transport in marine phytoplankton. *Eur. J. Phycol.* 38: 371-384.
930 <https://doi.org/10.1080/09670260310001612655>
- 931 60. Tikkanen M, Grebe S (2018) Switching off photoprotection of photosystem I - a novel tool for
932 gradual PSI photoinhibition. *Physiol. Plant.* 162: 156-161. <https://doi.org/10.1111/ppl.12618>
- 933 61. Tyystjärvi E (2013) Photoinhibition of Photosystem II. *Int. Rev. Cell Mol. Biol.* 300: 243-303.
934 <https://doi.org/10.1016/B978-0-12-405210-9.00007-2>
- 935 62. Van Steenkiste NWL, Stephenson I, Herranz M, Husnik F, Keeling PJ, Leander BS (2019) A new
936 case of kleptoplasty in animals: Marine flatworms steal functional plastids from diatoms. *Sci.*
937 *Adv.* 5(7):eaaw4337. <https://doi.org/10.1126/sciadv.aaw4337>
- 938 63. Vredenberg W (2015) A simple routine for quantitative analysis of light and dark kinetics of
939 photochemical and non-photochemical quenching of chlorophyll fluorescence in intact leaves.
940 *Photosynth. Res.* 124:87-106. <https://doi.org/10.1007/s11120-015-0097-x>
- 941 64. Wang QJ, Singh A, Li H, Nedbal L, Sherman LA, Govindjee, Whitmarsh J (2012) Net light-induced
942 oxygen evolution in photosystem I deletion mutants of the cyanobacterium *Synechocystis* sp.
943 PCC 6803. *Biochim. Biophys. Acta* 1817: 792-801. <https://doi.org/10.1016/j.bbabi.2012.01.004>
- 944 65. Yaakoubd B, Andersen R, Desjardins Y, Samson G (2002) Contributions of the free oxidized and
945 Q_B-bound plastoquinone molecules to the thermal phase of chlorophyll-*a* fluorescence.
946 *Photosynth. Res.* 74: 251. <https://doi.org/10.1023/A:1021291321066>
- 947 66. Zhang P, Eisenhut M, Brandt AM, Carmel D, Silén HM, Vass I, Allahverdiyeva Y, Salminen TA, Aro
948 EM (2012) Operon *flv4-flv2* provides cyanobacterial photosystem II with flexibility of electron
949 transfer. *Plant Cell* 24: 1952-71. <https://doi.org/10.1105/tpc.111.094417>

950

951

952

953

954 Figure legends

955 **Figure 1. Laboratory cultures of the photosynthetic sea slug *E. timida* and its prey alga *Acetabularia*.** A)

956 A freshly fed adult *E. timida* individual. The length of an adult slug in our culture conditions is
 957 approximately 6 mm. B) The giant-celled green alga *Acetabularia*. The cap-like structures are the site of
 958 gamete maturation and serve as indicators of the end of the vegetative growth phase of individual
 959 *Acetabularia* cells. The length of an individual *Acetabularia* cell at the end of the vegetative phase can
 960 reach 50 mm. C) The red morphotype *E. timida* can be induced by feeding it with red morphotype
 961 *Acetabularia*. Green morphotype *E. timida* individuals are also shown for reference. D) Red morphotype
 962 *Acetabularia* can be induced by subjecting the cells to cold temperature and high light (see “Materials
 963 and Methods” for details). E) *E. timida* and *Acetabularia* can be cultured in transparent plastic tanks. The
 964 two tanks in the foreground are *E. timida* tanks and the three other tanks contain *Acetabularia* cultures.

965 **Figure 2. Differences in Q_A^- reoxidation between *E. timida* (black) and *Acetabularia* (red) suggest**

966 **differences in the redox state of the PQ pool after dark acclimation.** A-C) Chlorophyll *a* fluorescence
 967 yield decay after a single turnover flash in aerobic conditions without any inhibitors in regular, green
 968 morphotypes of *E. timida* and *Acetabularia* (A), in aerobic conditions in the presence of 10 μ M DCMU
 969 (B), and in anaerobic conditions, achieved by a combination of glucose oxidase (8 units/ml), glucose (6
 970 mM) and catalase (800 units/ml), in the absence of inhibitors (C). See Figure 2 – figure supplement 1A
 971 for details on the anaerobic conditions. D) Chlorophyll fluorescence decay measured from the red
 972 morphotypes of *E. timida* and *Acetabularia* in aerobic conditions without any inhibitors. Fluorescence
 973 traces were double normalized to their respective minimum (measured prior to the single turnover
 974 flash), and maximum fluorescence levels. Curves in (A) are averages from 7 (*E. timida*) and 5
 975 (*Acetabularia*) biological replicates, 4 and 5 in (B), and 5 and 5 in (C-D), respectively. The shaded areas
 976 around the curves represent SE. All *E. timida* data are from individuals taken straight from the feeding
 977 tanks without an overnight starvation period. See Figure 2 – source data 1 for original data.

978 **Figure 3. Fluorescence induction kinetics during dark-to-light transition suggest differences in full**

979 **photochemical reduction of the PQ pool between *E. timida* (black) and *Acetabularia* (red).** A-C)
 980 Multiphase chlorophyll *a* fluorescence induction transient (OJIP) measured from dark acclimated *E.*
 981 *timida* and *Acetabularia* in aerobic conditions without any inhibitors (A), in the presence of 10 μ M
 982 DCMU (B), and in anaerobic conditions, achieved by a combination of glucose oxidase (8 units/ml),
 983 glucose (6 mM) and catalase (800 units/ml), without any inhibitors (C). Fluorescence traces were

984 normalized to their respective maximum fluorescence levels. For unnormalized data, see Figure 3 –
 985 figure supplement 1B. Curves in (A) are averages from 10 (*E. timida*) and 12 (*Acetabularia*) biological
 986 replicates, 10 and 9 in (B), and 13 and 11 in (C), respectively. The shaded areas around the curves
 987 represent SE. All *E. timida* data are from individuals taken straight from the feeding tanks without an
 988 overnight starvation period. See Figure 3 – source data 1 for original data.

989 **Figure 4. ECS and P700⁺ measurements indicate differences in proton motive force formation and**
 990 **utilization of alternative electron acceptors of PSI between dark acclimated *E. timida* (black) and**
 991 ***Acetabularia* (red) during a 780 ms high-light pulse.** A) ECS measured from *E. timida* and *Acetabularia*
 992 upon exposure to a high-light pulse in aerobic conditions. B) P700 redox kinetics upon exposure to a
 993 high-light pulse in aerobic conditions without any inhibitors. The inset shows P700 redox kinetics from
 994 the same samples during a second high-light pulse, fired 10 s after the first one. C) P700 oxidation
 995 kinetics in the presence of 10 μ M DCMU. D) P700 oxidation kinetics in the absence of DCMU in
 996 anaerobic conditions, achieved by a combination of glucose oxidase (8 units/ml), glucose (6 mM) and
 997 catalase (800 units/ml). The inset shows P700 oxidation kinetics from the same samples during the
 998 second high-light pulse. ECS and P700⁺ transients were double normalized to their respective dark levels
 999 (measured prior to the onset of the high-light pulse), and to the initial ECS or P700⁺ peak (measured
 1000 immediately after the onset of the pulse). Curves in (A) are averages from 13 (*E. timida*) and 6
 1001 (*Acetabularia*) biological replicates, 7 and 3 in (B), 13 and 4 in (C), and 8 (7 in inset) and 3 in (D),
 1002 respectively. The shaded areas around the curves represent SE. All *E. timida* data are from individuals
 1003 taken straight from the feeding tanks, without an overnight starvation period. See Figure 4 – source data
 1004 1 for original data.

1005 **Figure 5. P700 redox kinetics, photosynthetic electron transfer and photoprotective NPQ levels in *E.***
 1006 ***timida* kleptoplasts (left panels) are affected by the CO₂ acclimation state of its feedstock *Acetabularia***
 1007 **(right panels).** A-B) P700 redox kinetics in dark acclimated ambient-air (black) and high-CO₂ *E. timida*
 1008 (blue) (A) and ambient-air (red) and high-CO₂ *Acetabularia* (purple) (B) upon exposure to a 780 ms high-
 1009 light pulse. The ambient-air *Acetabularia* data are the same as in Figure 4B and are shown here for
 1010 reference. C-D) P700 redox kinetics during a second light pulse, fired 10 s after the first pulse, shown in
 1011 panels A-B, in ambient-air and high-CO₂ *E. timida* (C) and ambient-air and high-CO₂ *Acetabularia* (D). The
 1012 ambient-air *Acetabularia* data are the same as in Figure 4B inset and are shown here for reference. E-F)
 1013 RLC measurements from dark acclimated ambient-air (black solid line) and high-CO₂ *E. timida* (blue
 1014 dashed line) (E) and ambient-air (red solid line) and high-CO₂ *Acetabularia* (purple dashed line) (F).

1015 Illumination at each light intensity (PPFD) was continued for 90 s prior to firing a saturating pulse to
 1016 determine relative electron transfer rate of PSII (rETR). *E. timida* individuals used in RLC measurements
 1017 were fixed in 1 % alginate for the measurements (see “Materials and methods” and Figure 5 – figure
 1018 supplement 1 for details). G-H) Fluorescence traces and NPQ during the RLC measurements from
 1019 ambient-air and high-CO₂ *E. timida* (G) and ambient-air and high-CO₂ *Acetabularia* (H). P700⁺ transients
 1020 were double normalized to their respective dark levels and to the P700⁺ peak measured immediately
 1021 after the onset of the pulse. Curves in (A) are averages from 7 (ambient-air *E. timida*) and 8 (high-CO₂ *E.*
 1022 *timida*) biological replicates, 7 and 8 in (C), and 3 and 3 in (E,G), respectively. High-CO₂ *Acetabularia*
 1023 curves in (B,D) are averages from 3 biological replicates. Ambient-air and high-CO₂ *Acetabularia* curves
 1024 in (F,H) are averages from 3 biological replicates. Shaded areas around the curves and error bars show
 1025 SE. rETR and NPQ were calculated as described in “Materials and methods”. All *E. timida* individuals
 1026 used in panels (A,C,E,G) were allowed to incorporate the chloroplasts for an overnight dark period in the
 1027 absence of *Acetabularia* prior to the measurements. See Figure 5 – source data 1 for original data.

1028 **Figure 6. *Acetabularia* FLV levels in ambient air and high CO₂.** A) Densitometric quantification of
 1029 immunodetected FLV bands from *Acetabularia* grown in ambient air and high CO₂ conditions. Bars
 1030 indicate average protein levels and symbols show original data points. Student’s t-test indicated no
 1031 significant differences between the treatments (P= 0.594, n=3). B) Western blot used for protein
 1032 quantification in (A). FLV proteins were detected from total protein extracts using an antibody raised
 1033 against *C. reinhardtii* FLVB. The antibody reacts with both FLVA and FLVB proteins of *C. reinhardtii* (Jokel
 1034 et al., 2015). Wild-type *C. reinhardtii* (strain CC406) total protein extract was used as a positive control
 1035 and FLVA/B bands with their respective sizes are indicated. The lanes in (B) represent separate biological
 1036 replicates. Samples were loaded on total protein basis (25 µg protein/well). C) Coomassie stained
 1037 membrane from the blot in (B). See Figure 6 – source data 1 for original data of (B).

1038 **Figure 7. Altered P700 oxidation capacity does not affect chloroplast longevity in *E. timida* during**
 1039 **starvation in steady-light conditions.** A-B) Coloration of selected individuals (A) and body length (B) of
 1040 the ambient-air (black) and high-CO₂ *E. timida* (blue) slugs during steady-light starvation. The slug
 1041 individuals in (A) do not show the actual scale of the slugs with respect to each other. C-D) Maximum
 1042 quantum yield of PSII photochemistry (F_v/F_m) (C) and minimum (F_0) and maximum chlorophyll *a*
 1043 fluorescence (F_m) (D) during starvation in ambient-air (black) and high-CO₂ *E. timida* (blue). E) Second
 1044 pulse P700 oxidation kinetics after five days in steady-light starvation in ambient-air (black) and high-CO₂
 1045 *E. timida* (blue). Steady-light starvation light regime was 12/12h day/night and PPFD was 40 µmol m⁻²s⁻¹

1046 during daylight hours. See Figure 6 – figure supplement 1B for the spectra of lamps used in starvation
1047 experiments. All data in (B-D) represent averages from 50 to 8 biological replicates (see “Materials and
1048 methods” for details on mortality and sampling) and error bars show SE. P700⁺ transients in were double
1049 normalized to their respective dark levels and to the P700⁺ peak measured immediately after the onset
1050 of the pulse, and the curves in (E) represent averages from 7 (ambient air *E. timida*) and 5 biological
1051 replicates (high-CO₂ *E. timida*) and the shaded areas around the curves show SE. See Figure 7 – source
1052 data 1 for original data from panels B-E.

1053 **Figure 8. Higher P700 oxidation capacity protects the photosynthetic apparatus of ambient-air *E.***
1054 ***timida* during fluctuating-light starvation.** A-B) Maximum quantum yield of PSII photochemistry (F_V/F_M)
1055 (A) and minimum (F_0) and maximum chlorophyll fluorescence (F_M) (B) during fluctuating light starvation
1056 in ambient-air (black solid lines) and high-CO₂ *E. timida* (blue dashed lines). C-D) Second pulse P700
1057 oxidation kinetics after 0 and 5 days in fluctuating-light starvation in ambient-air (black) and high-CO₂ *E.*
1058 *timida* (blue). E-F) Relative electron transfer rate of PSII (rETR) (E) and NPQ (F) during RLC measurement
1059 from dark-acclimated ambient-air (black solid lines) and high-CO₂ *E. timida* (blue dashed lines) after 10
1060 days in fluctuating-light starvation. Illumination for each light step during the RLCs was continued for 90
1061 s prior to firing a saturating pulse to estimate rETR and NPQ. See Figure 8 – figure supplement 1 for the
1062 fluorescence trace and behaviour of NPQ during the RLC measurement. The light regime during the
1063 fluctuating light starvation was 12/12h day/night, and PPFD of the background illumination was 40 μmol
1064 $\text{m}^{-2}\text{s}^{-1}$, which was supplemented every 10 min with a 10 s high-light pulse during daylight hours. All data
1065 in (A,B) represent averages from 45 to 20 slug individuals (see “Materials and methods” for details on
1066 sampling). P700 redox kinetics in (C) represent averages from 9 biological replicates for both ambient-air
1067 and high-CO₂ *E. timida*, and 6 and 9 in (D), respectively. P700⁺ transients were double normalized to
1068 their respective dark levels and to the P700⁺ peak measured immediately after the onset of the pulse.
1069 Fluorescence based data in (E,F) represent averages of 5 biological replicates for ambient-air and high-
1070 CO₂ *E. timida*. All error bars and shaded areas around the curves show SE. See Figure 8 – source data 1
1071 for original data.

1072

1073

1074 Figure supplement legends

1075 **Figure 2- figure supplement 1. Oxygen consumption by the glucose oxidase system (8 units/ml glucose**
 1076 **oxidase, 6 mM glucose and 800 units/ml catalase) in room temperature.** A) Oxygen concentration in
 1077 250 ml of ASW medium inside a sealed bottle with minimal head space, stirred with a magnet, before
 1078 and after the addition of glucose oxidase. The arrow indicates the point where the last component of
 1079 the glucose oxidase system (glucose oxidase) was added into the mixture, after which the bottle was
 1080 sealed. B) Oxygen concentration in 2 ml of ASW medium in an open cuvette without any stirring. The
 1081 glucose oxidase system had been activated in a separate, sealed 5 ml vial 5 min prior to pipetting 2 ml of
 1082 the activated mixture into an empty measuring cuvette. Oxygen concentration in (A) and (B) was
 1083 measured with an optode-type oxygen meter FireStingO2 (PyroScience GmbH, Aachen, Germany) using
 1084 optically isolated oxygen sensor spots according to manufacturer's instructions.

1085 **Figure 3 – figure supplement 1. Technical considerations of the OJIP fluorescence induction**
 1086 **measurements.** A) Increasing the saturating pulse intensity from 50 % of the maximum (black solid line)
 1087 to 70 % (red dashed line) or 100 % (PPFD 3000 $\mu\text{mol m}^{-2}\text{s}^{-1}$; blue dash-dot line) in *E. timida*
 1088 measurements alters the O-J-I phases, but the intensity of the saturating pulse does not change the time
 1089 required to reach maximum fluorescence. The data for the saturating pulse intensity 70 % are taken
 1090 from Figure 3A. The curve for the 50 % saturating pulse represents an average from 12 biological
 1091 replicates, and a representative curve is shown for the 100 % intensity measurement, because raising
 1092 the saturating pulse intensity to >70 % often resulted in oversaturation of the fluorescence signal in *E.*
 1093 *timida*. B) Original, unnormalized fluorescence traces from the data shown in Figure 3A, representing
 1094 averages from 10 (*E. timida*) and 12 (*Acetabularia*) biological replicates. Shaded areas around the curves
 1095 represent SE. All *E. timida* data are from individuals taken straight from the feeding tanks, without an
 1096 overnight starvation period.

1097 **Figure 4 – figure supplement 1. ECS and P700⁺ signals from bleached *E. timida* individuals during a 780**
 1098 **ms high light pulse.** A) Bleached *E. timida* slugs were created by exposing them to one week starvation
 1099 in high light (Ikea Växer PAR30 E27, 10 W; PPFD>1000 $\mu\text{mol m}^{-2}\text{s}^{-1}$; 12/12h day/night cycle) in otherwise
 1100 normal growth conditions. B) ECS and C) P700⁺ signal from bleached slugs (black), measured using the
 1101 same protocol as with green slug individuals (green; data from Figures 4A and B are shown for
 1102 reference). ECS and P700⁺ transients were double normalized to their respective dark levels (measured
 1103 prior to the onset of the high-light pulse) and to the maximum signal immediately after the light pulse

1104 measured from the green slugs. Each curve from bleached slugs in (B) and (C) represents an average of 5
1105 biological replicates. The shaded areas around the curves represent SE. See Figure 4 – source data 2 for
1106 original data.

1107 **Figure 5 – figure supplement 1. The effect of alginate fixation on the maximum quantum yield of PSII**
1108 **(F_V/F_M).** Slug individuals were separately fixed in alginate and F_V/F_M was monitored before the fixation,
1109 immediately after the fixation, and after 5 and 10 min in fixation. The slugs had been in the dark for 20
1110 min before the first measurement and another 20 min dark period preceded the alginate fixation. The
1111 rest of the measurements were done at 5 min intervals, keeping the samples in the dark between the
1112 measurements. All data are averages from three biological replicates, and the error bars indicate SE.

1113 **Figure 7 – figure supplement 1. Normalized irradiance spectra from different light sources used in the**
1114 **study.** A) Growth light spectra, TL-D 58W/840 New Generation fluorescent tube (black) and Algaetron
1115 AG230 LED array (red), used as illumination in regular growth conditions and during acclimation to high
1116 CO_2 , respectively. B) Light sources used in the starvation experiments: Ikea Växer PAR30 E27, 10 W
1117 (black) was used for the starvation experiment in steady light; Heliospectra L4A greenhouse lamp was
1118 used for the starvation experiment in fluctuating light, and the spectra are from moderate light
1119 conditions (PPFD $40 \mu mol m^{-2}s^{-1}$; red) and during a high-light (HL) pulse (PPFD $1500 \mu mol m^{-2}s^{-1}$; blue).

1120 **Figure 8 – figure supplement 1. Fluorescence traces and NPQ during the RLC measurement.** All light
1121 steps of the RLC were continued for 90 s and the PPFDs used were 0, 11, 60, 100, 170, 270, 420 and 600
1122 $\mu mol m^{-2}s^{-1}$. The data represent averages of 5 biological replicates. All error bars and shaded areas
1123 around the curves show SE.

1124

1125

1126

1127

1128

1129

1130

1131

1132 [Figure source data](#)

1133 Figure 2 – source data 1

1134 Figure 3 – source data 1

1135 Figure 4 – source data 1

1136 Figure 4 – source data 2

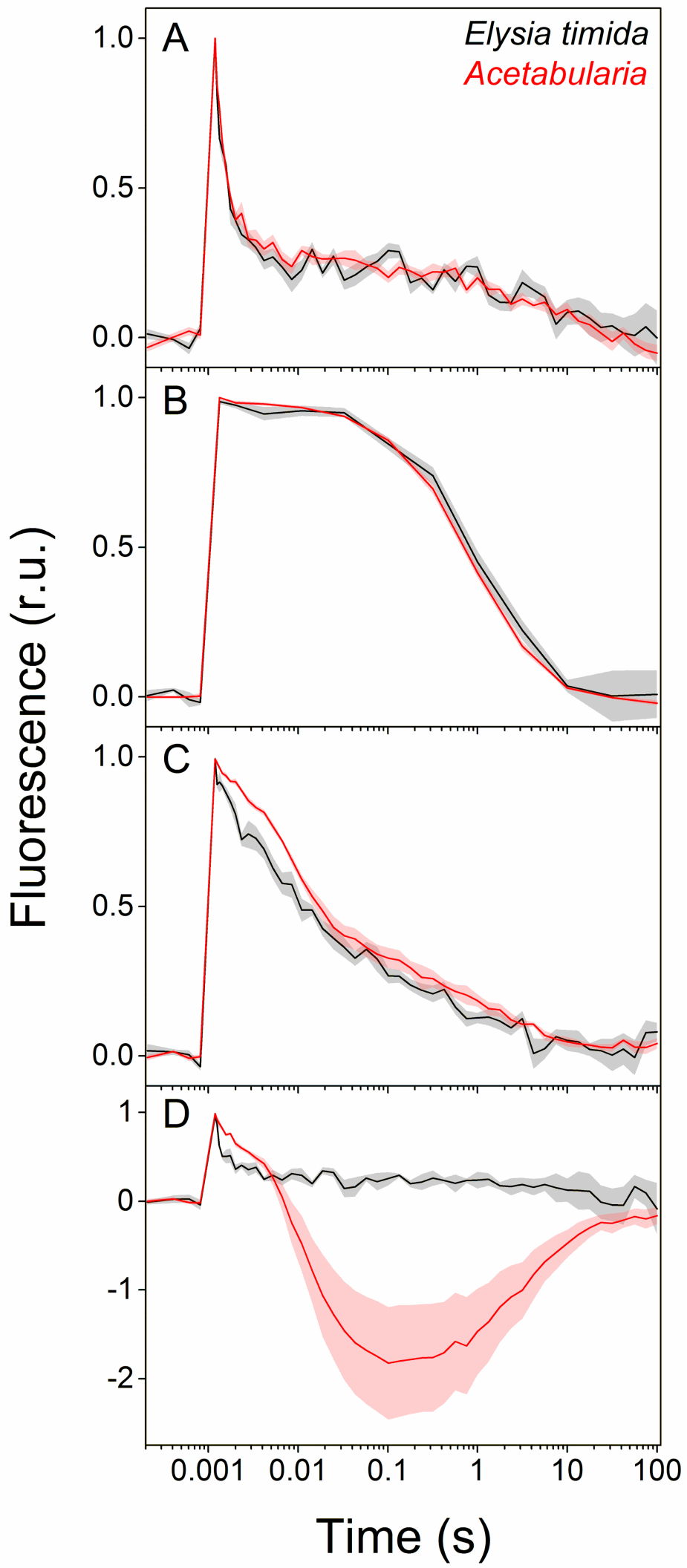
1137 Figure 5 – source data 1

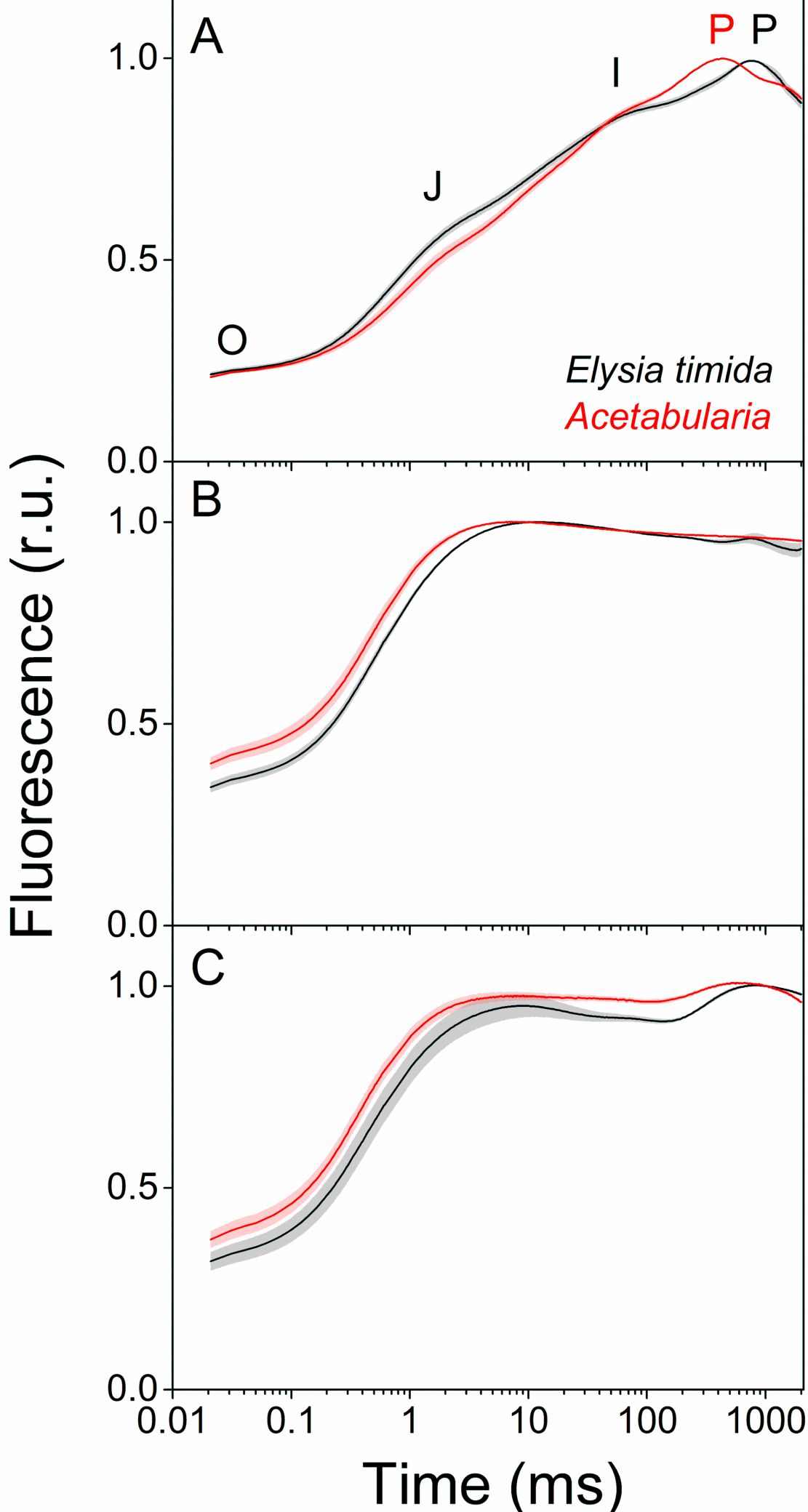
1138 Figure 6 – source data 1

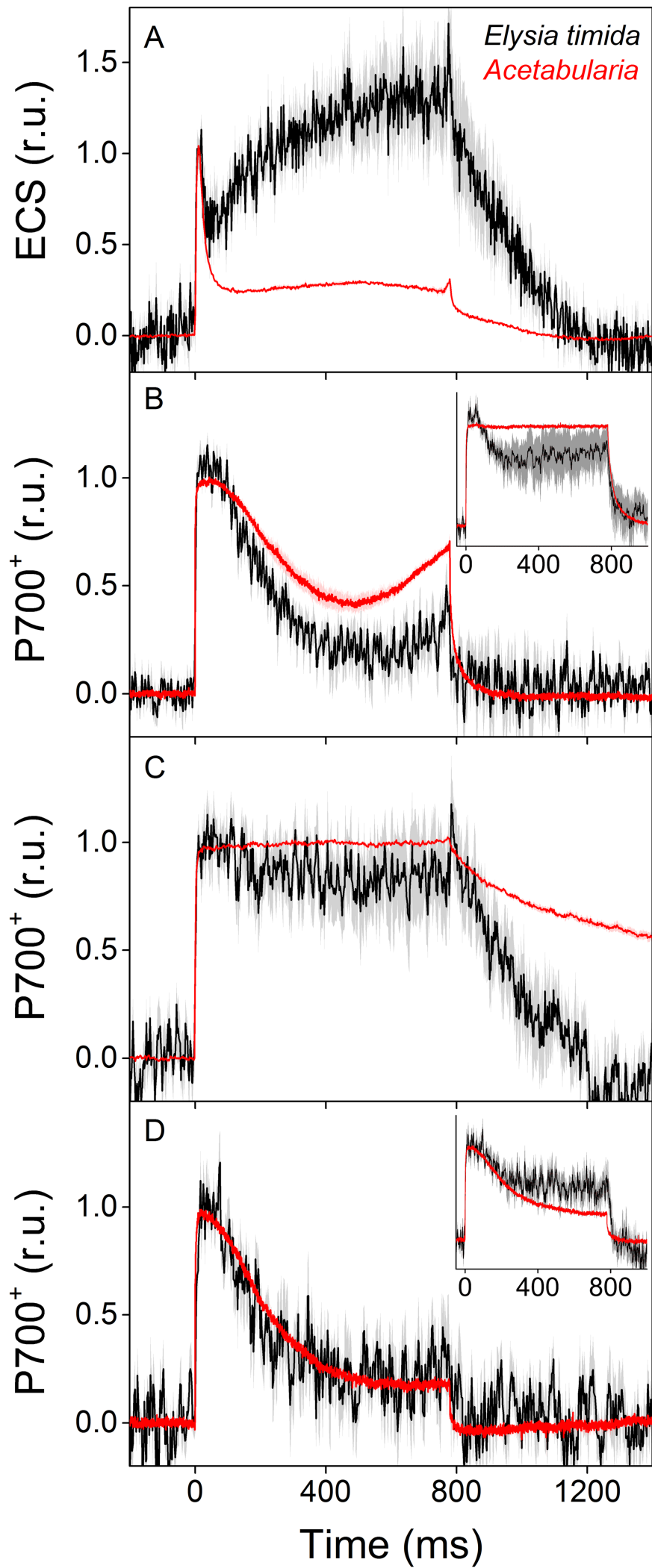
1139 Figure 7 – source data 1

1140 Figure 8 – source data 1

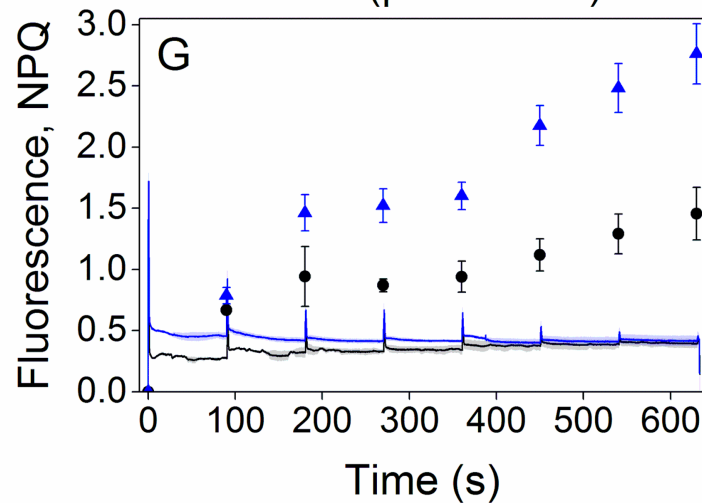
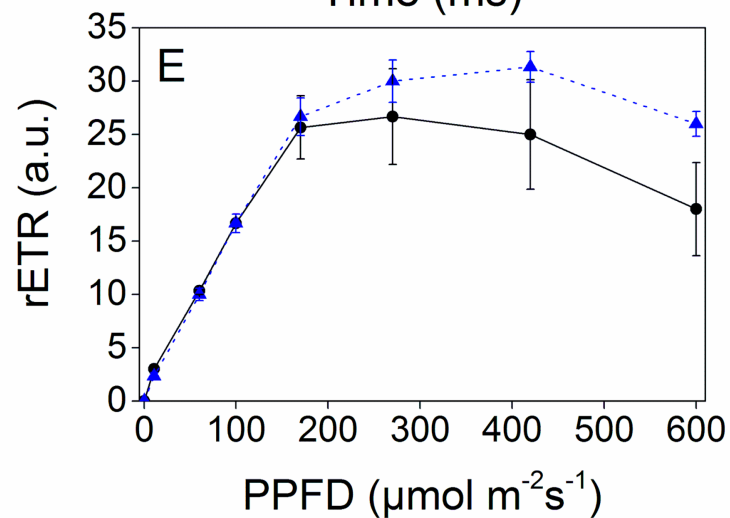
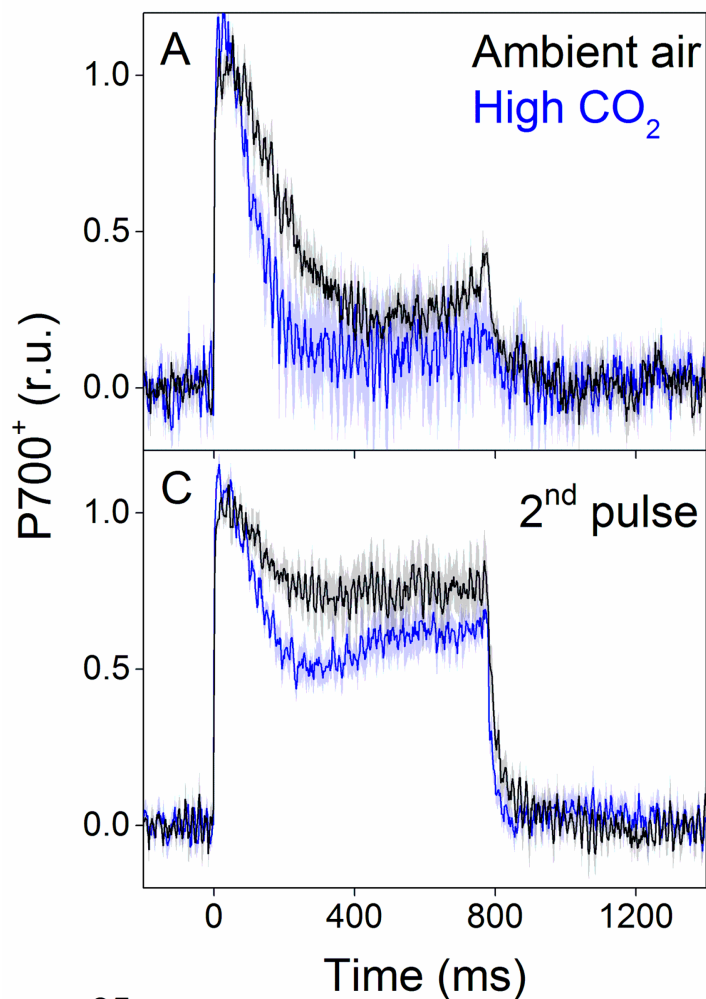




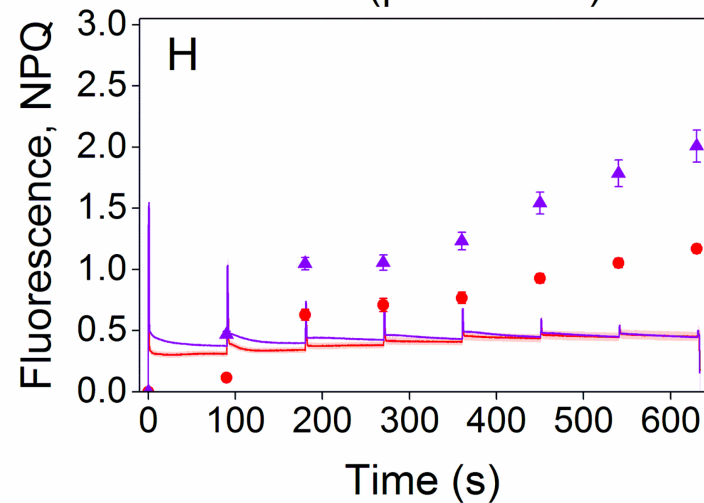
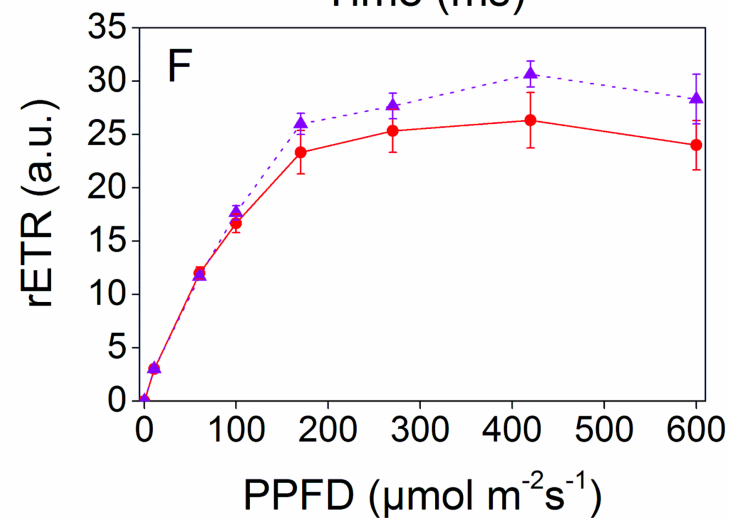
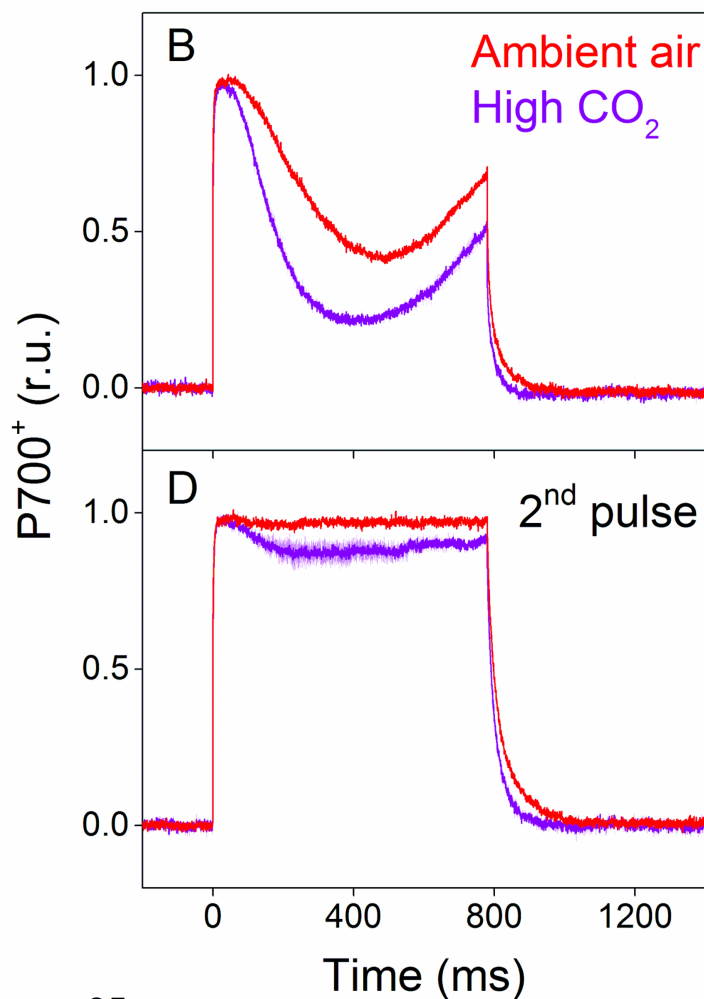


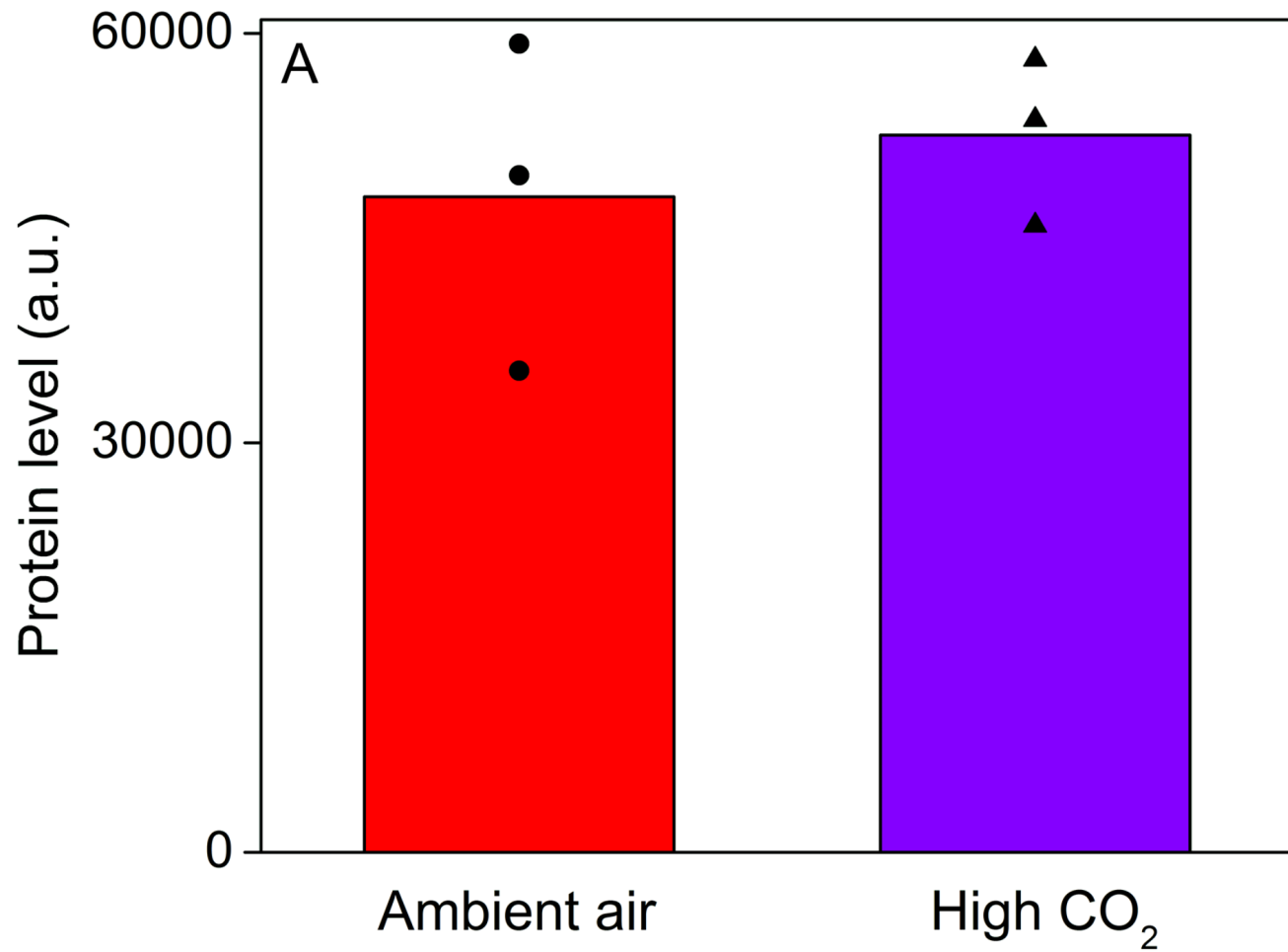


Elysia timida

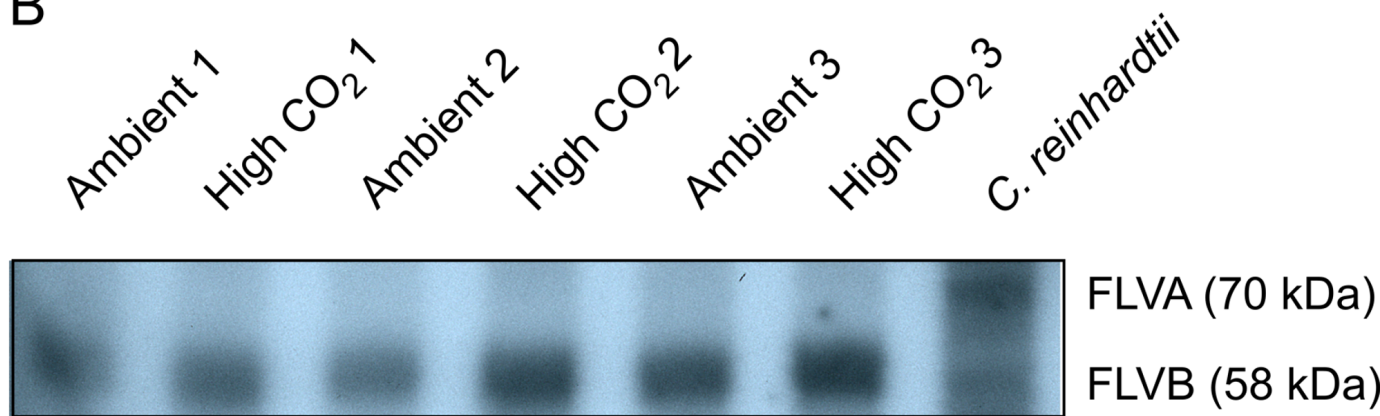


Acetabularia





B



C

